8-2016

Two-electron Quenching of Dinuclear Ruthenium(II) Polypyridyl Complexes

Yinling Zhang
University of Arkansas, Fayetteville

Two-electron Quenching of Dinuclear Ruthenium (II) Polypyridyl Complexes

A thesis submitted in partial fulfillment
of the requirements for the degree of
Master of Science in Chemistry

by

Yinling Zhang
Jilin University
Bachelor of Science in Chemistry, 2010
Jilin University
Master of Science in Chemistry, 2013

August 2016
University of Arkansas

This thesis is approved for recommendation to the Graduate Council.

_____
Dr. Bill Durham
Thesis Advisor

_____
Dr. Jingyi Chen
Committee Member

_____
Dr. Stefan Kilyanek
Committee Member

ABSTRACT

A bridging ligand 5,5'-Bi- 1,10-phenanthroline, diphen, was prepared using dichlorobis(triphenylphosphine)Ni(II), $Ni(PPh3)_2Cl_2$ as catalyst with a yield of 40%. Yellow cubic crystals were able to obtain from the good purity product for single crystal analysis. The torsion angle between the planes of the subunit phenanthrolines is about 66 degrees.

A dinuclear ruthenium (II) polypyridyl complex, $(phen)_2Ru(diphen)Ru(phen)_2^{4+}$, was synthesized by using polymeric ruthenium carbonyl compound as the entry point, diphen as the bridging ligand and 1,10-phenanthroline, phen, as the terminal legand. Brown needlelike crystals were precipitated from acetonitrile that were not suitable for single crystal diffraction.

The photochemistry of the dimer was investigated in regards to the oxidation and reduction of the ruthenium centers through a series of quenching reactions excited by visible light. The analogous monomeric complexes $Ru(bpy)_3^{2+}$ and $Ru(phen)_3^{2+}$ were used as comparisions. In the photoinduced oxidation with peroxydisulfate, $S_2O_8^{2-}$, the dimer showed a higher Stern-Volmer quenching constant k_q than $Ru(phen)_3^{2+}$. The dimer showed faster laser flash photolysis transients than $Ru(bpy)_3^{2+}$. In the photoinduced reduction with ascorbate, no significant difference between the dimer and $Ru(phen)_3^{2+}$.

ACKNOWLEDGEMENTS

I'd like to thank my research advisor Dr. Bill Durham for all his guidance and help he has given me during my time at University of Arkansas. I have been fortunate to have him as my savior, not only academically as well as physically and emotionally, who always was encouraging me, never putting me down. I sincerely thank him for his wisdom and supporting which helped me to finish this dissertation. I would also like to thank the Chemistry department in general for providing a great learning environment.

Thanks also to Dr. Jingyi Chen and Dr. Stefan Kilyanek for their willingness to serve on my graduate committee. Thanks to Dr. Nan Zheng for use of his lab. I would also want to thank Dr. Latisha Puckett who is the past member of the Durham's research group for her help.

I am grateful to my friends and colleagues for their encouragement and moral support which made my stay and studies in Fayetteville more unforgettable.

Most of all, I would like to thank my lovely parents for all the understanding, patience, love, and support that they has given me during my studies.

TABLE OF CONTENTS

LIST OF TABLES AND FIGURES

Figure 4.1 Left: The model of the diphen single-crystal structure. Anions are omitted for clarity. Atom color code: carbon, grey; nitrogen, blue. Right: The structure for phen⋯⋯⋯⋯100

Chapter 1 Introduction

1.1 Introduction

In 1839 French physicist Edmond Becquerel showed that photoelectric conversion was possible by generating a current with the first photovoltaic cell[1]. The cell consisted of layer of silver chloride placed in an acidic solution along with a platinum electrode. Modern photovoltaic devices are based primarily on semiconductor electrodes. These devices suffer from relatively high costs and low light-to-electric energy conversion efficiency. Many alternative devices are also being developed. Dye sensitized solar cells offer some advantages over solid state devices. They are potentially less expensive but suffer from poor stability among other things. In 1991, Michael Grätzel and Brian O'Regande reported a low-cost dye solar cell (DSC) based on a layer of the trimeric ruthenium complex, $[Ru(bpy)_2(CN)_2]_2Ru(bpy(COO)_2)_2^2$. The conversation efficiency of the early cell was above 7 %.

Figure 1.1 is a schematic diagram of typical dye sensitized solar cell. In these cells the light is absorbed by the dye. The excited dye molecule transfers an electron to the TiO_2 semiconducting electrode. This forms the negative side of the cell much like an ordinary battery. The positive side involves the conversion of I_3^- to $3I^-$ by way of the returning flow of electrons. The structure of two of the most popular ruthenium based dyes is illustrated in Figure 1.2. The use of ruthenium(II) complexes containing polypyridyl ligands is a common theme and will be discussed in more detail shortly.

Fig 1.1 Schematic of electron pathway in a DSC system[3]

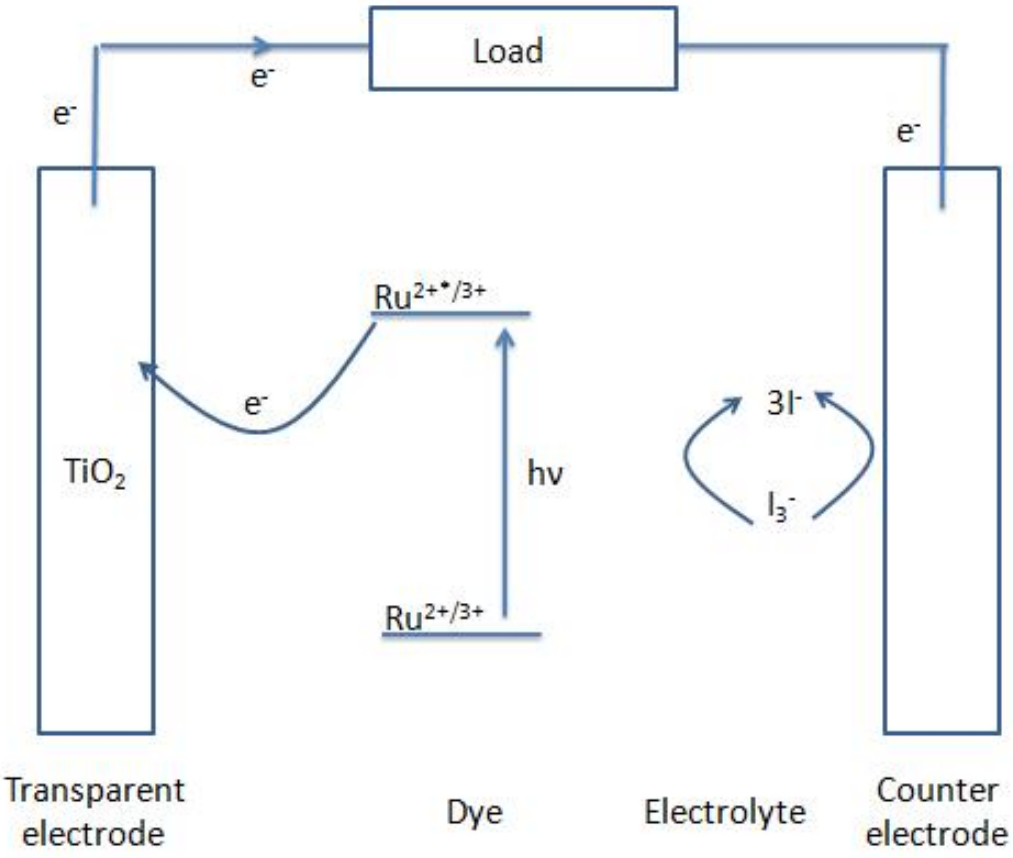
Load
e-
e-
e-
Ru2+*/3+
e-
TiO2
hv
Ru2+/3+
3I-
I3-
Transparent electrode
Dye
Electrolyte
Counter electrode

Fig.1.2 Structure of ruthenium based N-3 dye and thoicyanate-free dye

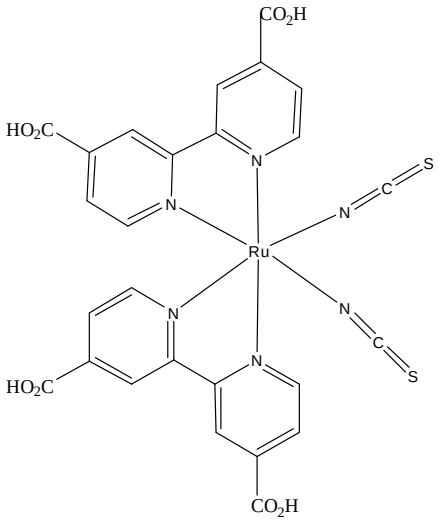
CO2H
HO2C
N
N
Ru
N
C
S
N
C
S
N
N
HO2C
CO2H

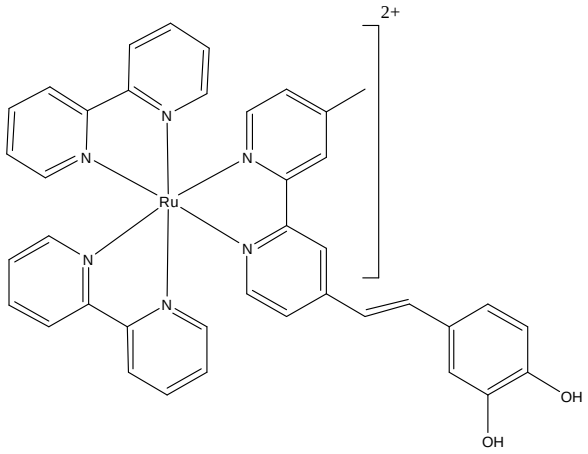
2+
N
N
Ru
N
N
N
N
OH
OH

1.2 Conversion of Solar Energy to Alternative Fuels

Photovoltaic conversion of light into energy is one of many ways to capture solar energy.[4] From a purely energetics standpoint it should be possible to use an appropriate dye to convert water into hydrogen and oxygen.[5] The possibility is very appealing and many investigators have examined this problem. The ruthenium (II) complex containing three bipyridine ligands, $Ru(bpy)_3^{2+}$, was among the first dyes extensively examined in this context.[6] Unfortunately, despite a considerable effort the goal remains elusive.

One of the major stumbling blocks in the proposed application is the fact that the conversion of water to O_2 requires 4 electrons. The ruthenium complex is only capable of providing one electron for each photon absorbed. Unfortunately, the energetics of the process becomes unfavorable if the electrons can only be transfer one at a time because of the formation of high energy intermediates.[7] The conversion of water to hydrogen likewise requires 2 electrons. Several researchers have tried using platinum based catalysts[8] to collect electrons and convert water to hydrogen at the electrode surface.

1.3 Photophysical and Redox Properties of Ruthenium (II) Complexes

Ruthenium complexes have played a central role in a large variety of energy conversion schemes and photosensitive devices because of the unique set of characteristics.[4, 9] Ruthenium (II) forms a variety of polypyridyl coordination complexes. These complexes were first discovered almost 80 years ago.[10] The simplest and most well-known complex of this family is $(bipyridine)_3Ru(II)$ or $Ru(bpy)_3^{2+}$, which has played a central role in the development of photochemical applications due to its remarkably chemical stability and its unique photo-physical properties[11]. These properties have been applied to a variety of applications, such as artificial photosynthesis, photocatalytic production of hydrogen, dye-sensitized solar cells,

photon-induced switches, oxygen sensors, pH sensors, and molecular machines and devices. The Ru-ligand coordination is very strong. For example, $Ru(bpy)_3^{2+}$ remains unreacted after refluxing in concentrated HBr. In addition, Ru(I), Ru(II) and Ru(III) complexes retain the bipyridyl coordination sphere.[12] This property is rare across the periodic table and critically important for sustained catalytic activity and electrochemically reversible redox processes (the $Ru^{1+/2+}$ and $Ru^{2+/3+}$ processes). These important electronic and photophysical properties are retained in hundreds of structurally modified derivatives of the parent complex. Such structural modifications enable researchers to tune both the properties for specific applications

The absorption and emission spectrum of $Ru(bpy)_3^{2+}$ is shown in Fig.1.3. The bands at 185 nm and 285 nm are assigned as ligand-centred $\pi \rightarrow \pi^*$ transitions by comparison with the spectrum of the protonated bipyridine ligand[13]. Similarly, the two weak shoulders at 323 nm and 345 nm also with the twin peaks at 238 nm and 250 nm are assigned to the metal centred $d \rightarrow d$ transitions. The two intense bands at 240 nm and 450 nm which located in visible light range are spin-allowed MLCT $d \rightarrow \pi^*$ transitions. $Ru(bpy)_3^{2+}$ shows a broad orange-yellow emission in solution at 293 K around 600 nm, and the rate of decay corresponds to an excited state lifetime approximately 600 nsec in aqueous solution at room temperature in the absence of oxygen.[14]

Fig.1.3 Absorption and emission spectrum for $Ru(bpy)_3^{2+}$ in aqueous solution at room temperature along with the assignments for the various bands.

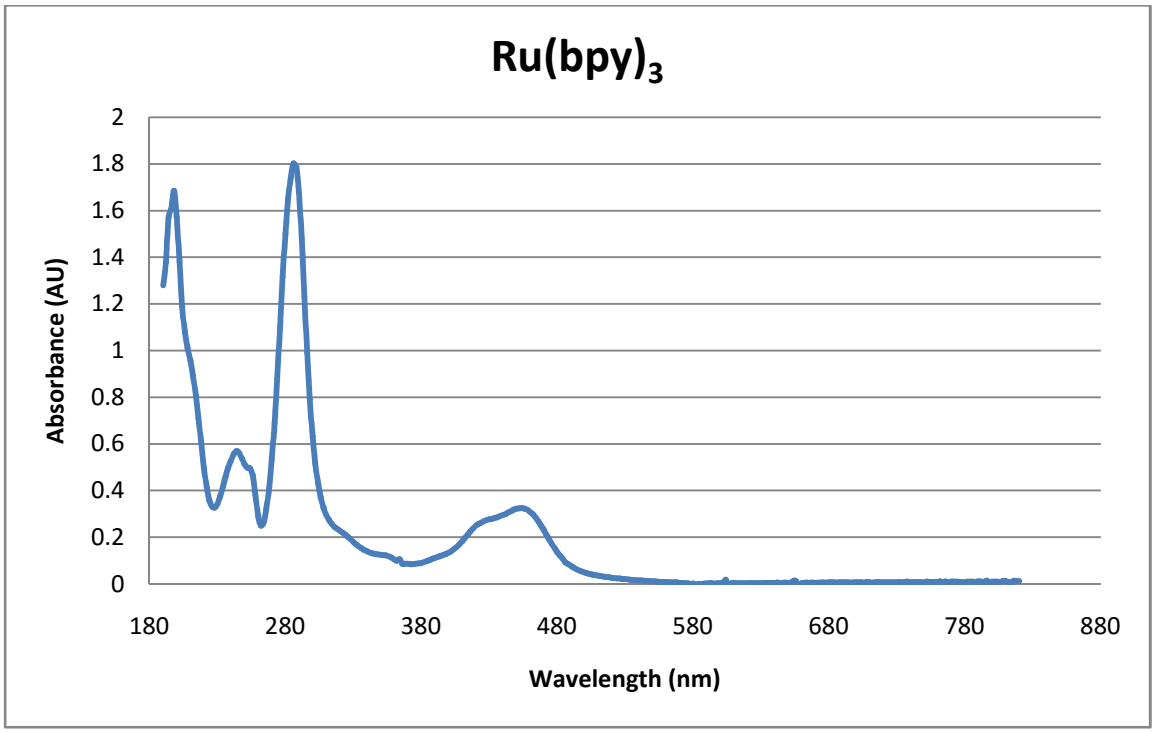
Ru(bpy)3
Absorbance (AU)
2
1.8
1.6
1.4
1.2
1
0.8
0.6
0.4
0.2
0
180
280
380
480
580
680
780
880
Wavelength (nm)

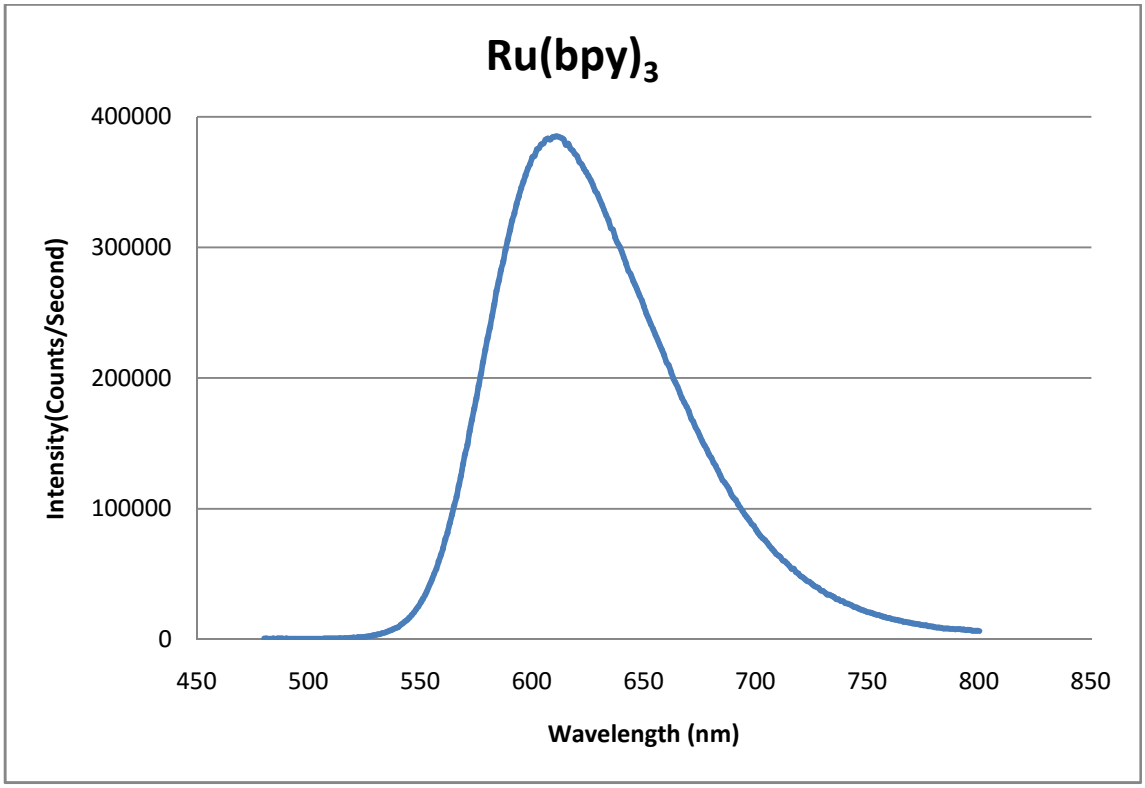
Ru(bpy)3
Intensity(Counts/Second)
400000
300000
200000
100000
0
450
500
550
600
650
700
750
800
850
Wavelength (nm)

Fig. 1.4 Excited-state decay pathway for $Ru(bpy)_3^{2+}$

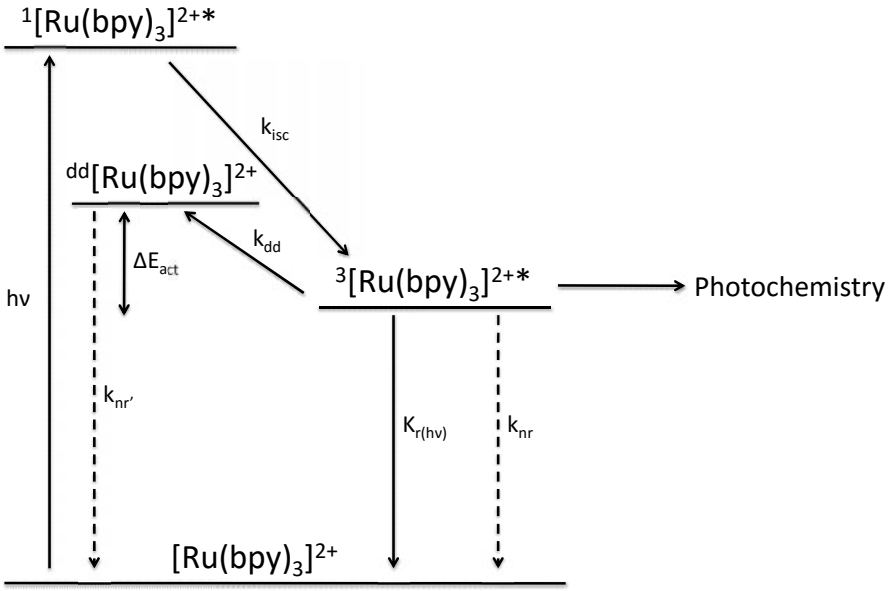
$^1[Ru(bpy)_3]^{2+*}$
k_{isc}
$^{dd}[Ru(bpy)_3]^{2+}$
k_{dd}
ΔE_{act}
$^3[Ru(bpy)_3]^{2+*}$
Photochemistry
hv
$k_{nr'}$
$K_{r(hv)}$
k_{nr}
$[Ru(bpy)_3]^{2+}$

The excited state decays involve several processes (Fig 1.4). By irradiating Ru complexes, for example $[Ru(bpy)_3]^{2+}$, at the appropriate wavelength, a lowest photoexcited singlet metal-to-ligand charge transfer state (^{1}MLCT) is produced, $^1[Ru(bpy)_3]^{2+}*$, which then undergoes intersystem crossing (k_{isc}) within 300 fs[15], yielding a long-lived luminescent triplet excited state (^{3}MLCT), $^3[Ru(bpy)_3]^{2+}*$ (600 ns to a few μs). The intersystem crossing yield in the few system examined in detail is approximately 100%. This excited state exists long enough to transfer energy to another molecule by energy transfer or electron transfer. $^3[Ru(bpy)_3]^{2+}*$ can also relax to the ground state through a non-rediative decay (k_{nr}) by emission of heat, or a radiative decay (k_r) by emission of light at about 600 nm, or thermal population of the nearby metal-centered d-d state, $^{dd}[Ru(bpy)_3]^{2+}$. The d-d state rapidly decays back to the ground state and is the primary decay path for the excited state in the absence of other reagents.[16]

$Ru(bpy)_3^{2+}$ in ground state tends to show no redox reactions. Once in excited state, however, $Ru(bpy)_3^{2+}*$ can behave as both a strong oxidant or a strong reductant. One-electron transfer reactions result in the formation of ground state Ru(III) that is a strong oxidant (+1.29 V vs SCE in CH_3CN) or the formation of ground state Ru(I) a very strong reductant (-1.33 V vs SCE in CH_3CN). The standard reduction potentials for the ground and excited state of $Ru(bpy)_3^{2+}$ are summarized in Figure 1.5.[17]

Fig. 1.5 Photoredox cycles of $Ru(bpy)_3^{2+}$

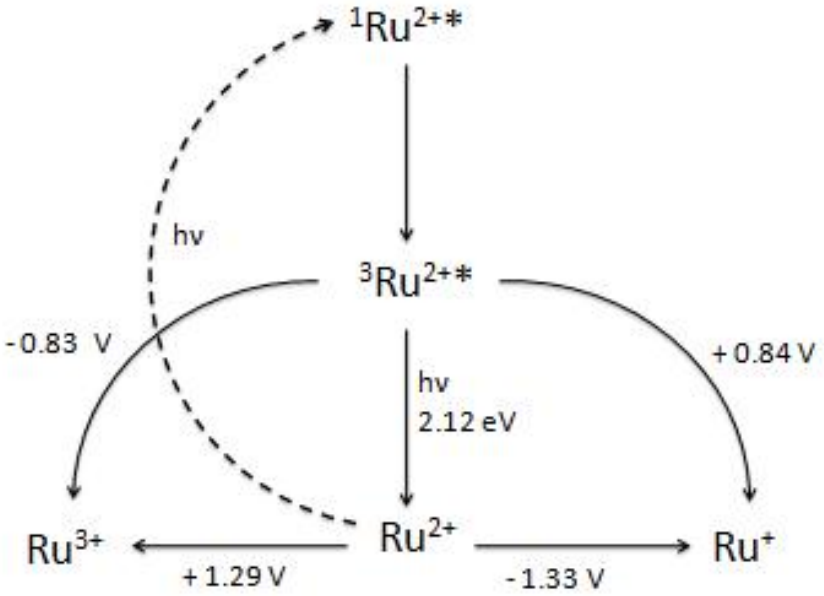
$^1Ru^{2+*}$
hv
$^3Ru^{2+*}$
-0.83 V
+0.84 V
hv
2.12 eV
Ru^{3+}
Ru^{2+}
Ru^{+}
+1.29 V
-1.33 V

1.4 Applications of Ruthenium (II) Complexes and Laser Flash Photolysis

The redox properties of the excited states ruthenium polypyridyl complexes have led investigators to many applications. Of particular importance is the ability to monitor the rates of the electron transfer reactions.[18] For several decades this ability has dominated the fundamental investigations of electron processes. Most notable was the verification of the basic tenants of Marcus Theory and development of basic understanding of electron transfer in metalloproteins and other systems in which the donor and acceptor are separated by significant distances.[19]

1.4.1 Laser Flash Photolysis

Laser flash photolysis has been used extensively to measure the rates of electron transfer reactions involving ruthenium polypyridyl complexes.[20] The technique is extremely well suited for these investigations. Laser flash photolysis allows for the measurement of reactions with almost no limit of the time resolution. Femotosecond measurements are currently common although most practical applications focus on reactions that occur in the microsecond or millisecond time range.[21] The technique is based on the creation of reactants by using a short pulse of light. Typically, lasers have pulse widths in the nanosecond or picosecond range are able to produce reactants on this time scale. The pulse width is generally much shorter than the half-time of the chemical reaction. A simplified optical layout of the essential equipment is shown in Figure 1.7.

Most flash photolysis system use absorbance measurements to monitor the reaction. Transient absorbance changes are recorded on a fast digital oscilloscope (nsec sampling). Ruthenium complexes have excited states that last long enough to produce a good yield of product. Excitation and monitoring can be done with visible light which is best for most systems.

Fig 1.6 Essential optical layout of a laser flash photolysis setup

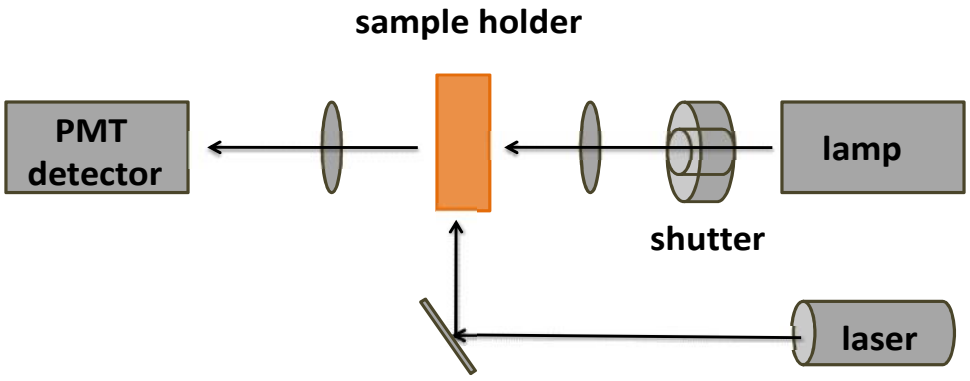
sample holder
PMT
detector
lamp
shutter
laser

1.4.2 Reactions Between Ruthenium(II) Complexes and Proteins (Ru(II)-Fe(III))

The process of aerobic cell respiration is a one of the most complicated and interested processes because it actually consists of many individual electron transfer reactions. The final step in respiration is called oxidative phosphorylation which takes place on the electron transport chain of the inner membrane of the mitochondria.[22]

The electron transport chain is a series of proteins: complex I (or NADH dehyrogenase), complex II (succinate reductase), complex III (or cytochrome bc_1 complex)[23] and complex IV (or cytochrome c oxidase), as well as the final protein molecule known as ATP synthase.

Complex I is responsible for accepting the high energy electrons from NADH molecules produced in glysolysis and the citric acid cycle to ubiquinone. As the electrons move through complex I, four proton ions are pumped out the matrix into the inner membrane. Complex II converts succinate to fumarate and generates the $FADH_2$ molecules without pumping any proton ions. Ubiquinone is the electron carrier that shuttles these electrons from complex I and II onto complex III. Then complex III catalyzes the transfer of electrons from ubiquinone to cytochrome c.[24] The movement of electrons stimulates the movement of proton ions out of the matrix and into the inner membrane space of the mitochondria. Once the electrons end up on complex IV, this is where the diatomic oxygen is reduced by the electrons to form water. This series of reactions yields a proton gradient that is used by ATP synthase to generate ATP molecules.

Fig 1.7 Structure of a mitochondrion

Fig 1.8 Mitochondrial electron transport chain

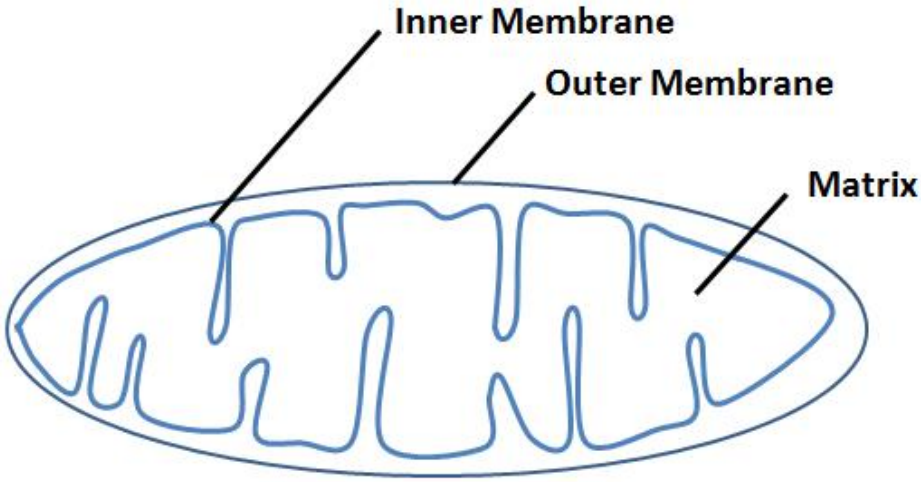
Inner Membrane
Outer Membrane
Matrix

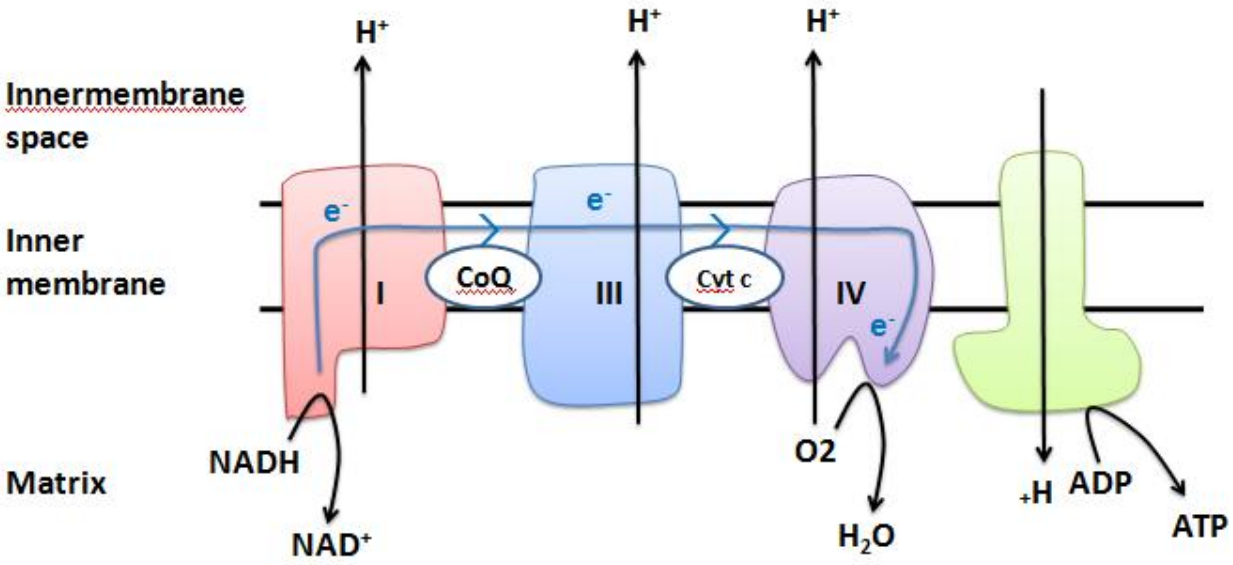
Innermembrane space
Inner membrane
Matrix
H+
H+
H+
e-
e-
e-
I
CoQ
III
Cyt c
IV
NADH
NAD+
O2
H2O
+H
ADP
ATP

During the process of this oxidation, cytochrome c is a relatively small water soluble molecule travels through the matrix fluid plays a crucial role as a one-electron shuttle between complex III and IV[25]. Cytochrome c contains a single iron atom held by four nitrogens of a porphyrin ring, the nitrogen of histidine, and the sulfur atom of methionine. The iron atom is center of the redox activity and cycles between Fe(II) and Fe(III) form to accept one electron from Complex III and subsequently donate one electron to Complex IV.

Measurement of the rate constants for electron transfer within the oxidative phosphorylation remained elusive until early 1900's because of the speed of the reactions. Rapid mixing techniques fell far short of the needed time resolution and flash-photolysis was not directly possible redox reactions could not be initiated by irradiation of the proteins alone. In early 1990, use of laser flash photolysis became possible through photoexcitation of ruthenium polypyridine complexes.[26]

In the early research, ruthenium complexes were covalently bound to cytochrome c[27]. Ru(II)-Fe(III) in Scheme 1.1 represents ruthenium complexes and the iron center of cytochrome c. Absorption of a short laser pulse leads to the formation of the Ru^{2+}* excited state, which rapidly reduces the iron center to produce Ru(III)-Fe(II). The use of an external sacrificial electron donor, D, prevents the thermal back reaction with the formation of Ru(II)-Fe(II). At this point the reduced cytochrome c can react with a metalloprotein of interest (cytochrome c oxidase, cytochrome peroxidase) after which the ruthenium components are reset to their original oxidation states.

Subsequent research revealed that covalent bonding was not necessary for many of the questions under investigation. Electrostatic interactions with the ruthenium complexes with a

metalloprotein of interest, when correctly designed, provided good yields of proteins in reactive states. For examples, this approach worked very well in studies of the internal electron transfer reactions of multicentered metalloproteins such are Complex III and IV. In these applications the ruthenium complex essentially replaced cytochrome c as an electron donor or acceptor. Extensive design efforts ultimately showed that weakly coupled dimeric ruthenium complexes worked best. For example, the complex $[(bpy)_2Ru\text{-}qpy\text{-}Ru(bpy)_2]^{4+}$, where qpy is quatrapyridine was used extensively to examine the internal electron transfer reactions of cytochrome c oxidase.[28]

Scheme 1.1 Photoredox reaction of ruthenium in the presence of external quenchers

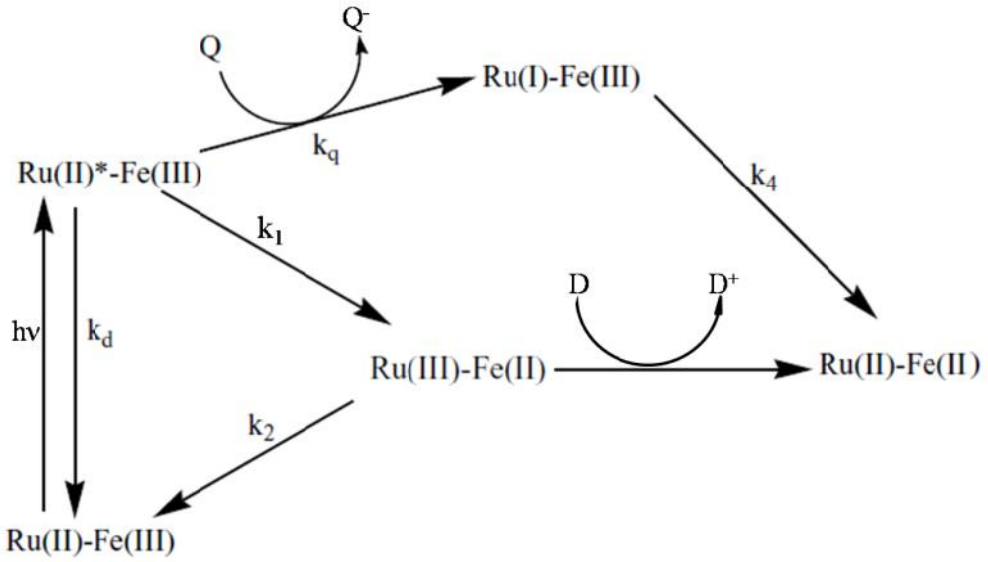
Q
Q⁻
Ru(I)-Fe(III)
k_q
Ru(II)*-Fe(III)
k_4
k_1
D
D⁺
hν
k_d
Ru(III)-Fe(II)
Ru(II)-Fe(II)
k_2
Ru(II)-Fe(III)

1.4.3 Light-driven Oxidation of Water Catalyzed by Ruthenium (II) Complexes

Oxidation of water to release O_2 is the terminal reaction of green plants, photosystem II (PSII) (eq 1) .[29] Oxidation of water is extremely energy-demanding and occurs thermodynamically above pH ~ 5 with potentials, $E^0(O_2/H_2O_2) = 0.27$ V, $E^0(H_2O_2/H_2O) = 1.36$ V) (eq 2) .[30] There are very few suitable molecules that can oxidize water by absorbing the energy from sunlight as it happens in the photosynthesis in green plants. However ruthenium (III) complexes have this ability, for example $Ru(bpy)_3^{3+}$. [31]

$$2H_2O = 4H^+ + O_2 + 4e^- \qquad (1)$$

$$Ru(bpy)_3^{3+} + ½\ H_2O = Ru(bpy)_3^{2+} + H^+ + ¼\ O_2 \qquad (2)$$

$Ru(bpy)_3^{2+}$ absorbs visible light to form the MLCT excited state $Ru(bpy)_3^{2+}$*. Then $Ru(bpy)_3^{2+}$* is oxidized by an appropriate oxidative quencher such as $S_2O_8^{2-}$ to $Ru(bpy)_3^{3+}$. By accepting electrons from water, water is oxidized to O_2 and $Ru(bpy)_3^{3+}$ is reduced and returns back to the initial state $Ru(bpy)_3^{2+}$.

However, the evolution of O_2 from water is difficult in this four-electron redox process and $Ru(bpy)_3^{3+}$ decomposes rapidly. More research is need to develop more efficient and practical photosensitizer for water oxidation that could meet the following requirements: a high turnover number which reflects high stability; a high turnover frequency which reflects high activity and a low overpotential which means water oxidation can be driven by visible light[32].

Fig 1.9 Photocatalytic oxidation of water by $Ru(bpy)_3^{2+}$.

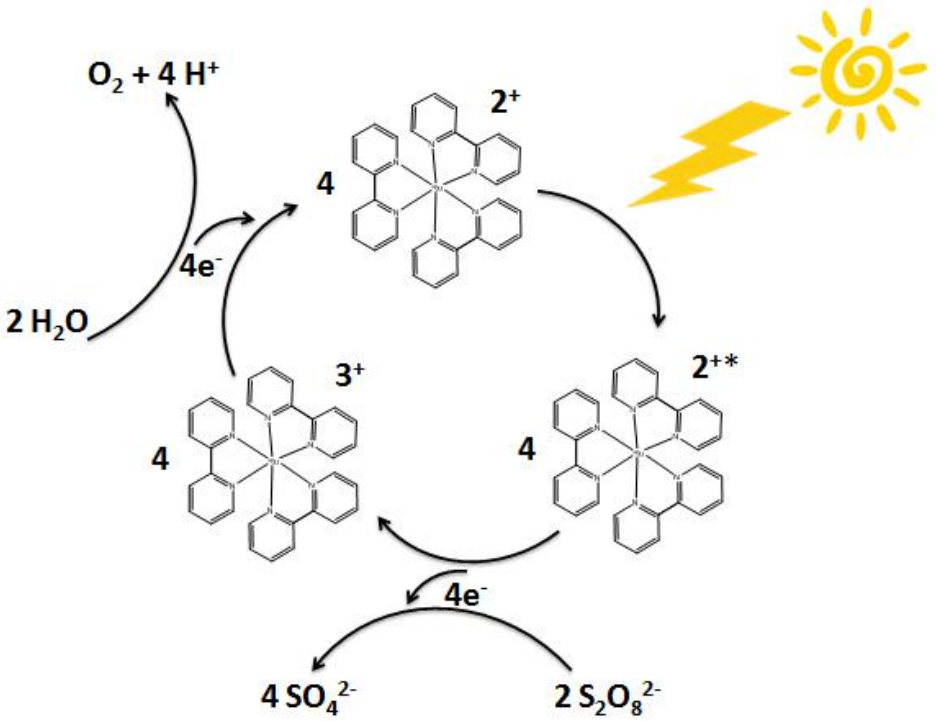
O2 + 4 H+
2 H2O
4e-
4
2+
2+*
4
3+
4
4e-
4 SO4 2-
2 S2O8 2-

1.4.4 Organic Synthesis Using Visible-light Triggered by $Ru(bpy)_3^{2+}$

Sunlight is inexpensive and endlessly renewable. Photosynthesis in green plants serves as natural ability to convert solar energy to chemical energy. This green chemistry has inspired the development of photoredox catalysts for organic synthesis. However, most organic catalysts absorb short wavelengths of light[33], for example ultraviolet light which is reactive for unsaturated bonds and some functional groups makes up asmall amount (~3%) of sunlight. By utilizing the properties of ruthenium polypyridine complexes, strategies using combination of $[Ru(bpy)_3]^{2+}$ and visible light for preparative organic chemistry haverecently been developed.

Fig 1.10 Examples for organic photosensitizers absorb ultraviolet light

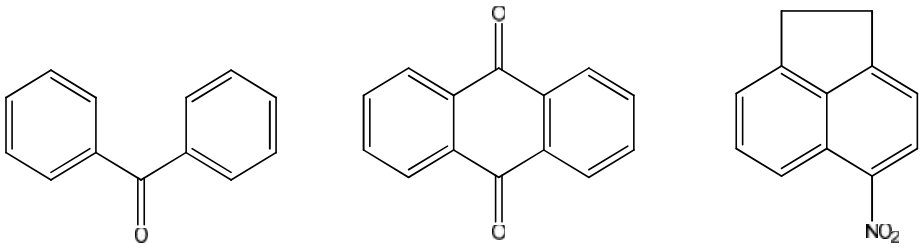

Benzophenone (BP) Anthraquinone (AQ) 5-Nitroacenaphthen (NAN)

Scheme 1.2 Traditional method for reductive dehalogenation

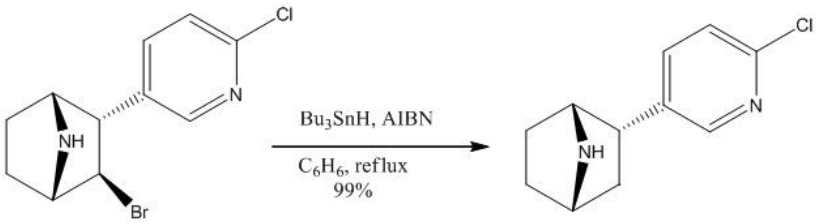

Scheme 1.3 Photoredoxmethod for reductive dehalogenation

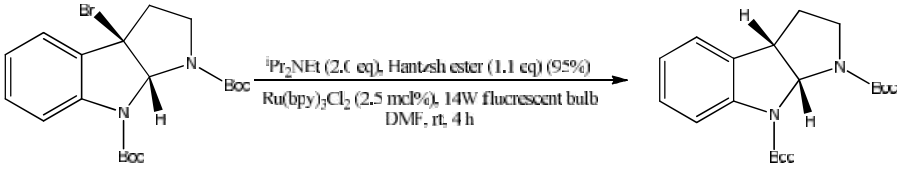

Scheme 1.4 Photoredox reduction of electron-deficient olefins

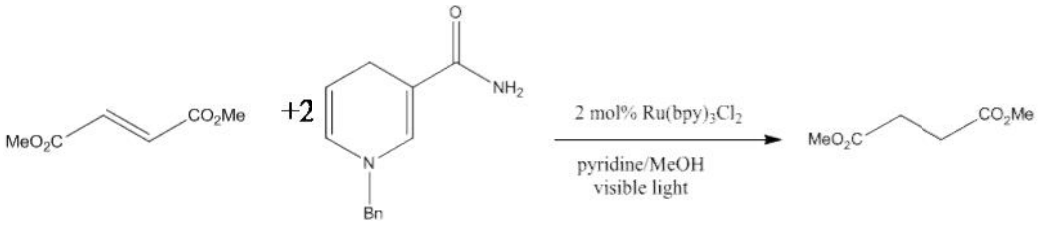

Reductive dehalogenation is degradation of halogenated organic compounds by removal of a halogen substituent and simultaneous addition of a hydrogen atom. An example of commonly used traditional method is shown in Scheme 1.2 which involves trialkyltinhydride compound as the catalyst[34]. However, trialkyltin is neurotoxic can cause impaired motor function[35]. Subsequently a tin-free method using $[Ru(bpy)_3]^{2+}$as a visible-light photosensitizer irradiated by a 14 W fluorescent lamp under mild reaction conditions was developed (Scheme 1.3)[36]. This simply reaction maintained good chemoselectivity and high yields of products.

$[Ru(bpy)_3]^{1+}$ is a strong reductant can reduce some electron-deficient olefins. No reaction between several olefins and 1-benzyl-1, 4-dihydronicotinamide (BANH) is observed in the dark at room temperature. By adding catalytic quantities of $[Ru(bpy)_3]^{2+}$ and under visible light, the excited state $Ru(bpy)_3^{2+}$* was formed and was reduced by accepting an electron from BANH to generate highly reducing $Ru(bpy)_3^{1+}$. $Ru(bpy)_3^{1+}$ reduced the carbon-carbon double bond to single bond(Scheme 1.4) .[37]

$Ru(bpy)_3^{2+}$ has been investigated for more than four decades.[38] However, the utilizing of $Ru(bpy)_3^{2+}$ to trigger organic synthesis started in 2008.[39] This is a new area in advanced organic synthesis and catalysis but application examples are still limited.

1.5 Two and Four-electron Donors and Acceptors

In some of the examples above it is clear that development of catalysts capable of delivering more than a single electron per photon would be beneficial. Direct 2-photon processes occur with low yields and only with an extremely high photon flux. Alternatively dimeric complexes can be envisioned in which the metal centers are very weakly coupled. In this case the metal centers would behave independently and it should be possible to excite both

centers with only modern levels of photon flux. In this case the probability of absorbing a second photon would be the same as absorbing the first photon.

Several dimeric ruthenium complexes have recently been developed that fit the criteria of weakly coupled metal centers. One has been used extensively in the investigation of metalloproteins and was mentioned above, $[(bpy)_2Ru\text{-}qpy\text{-}Ru(bpy)_2]^{4+}$.[28] Another is closely related and easier to prepare, $[(phen)_2Ru\text{-}diphen\text{-}Ru(phen)_2]^{4+}$. In both of these dimers the bridging ligands are sterically constrained out of planarity and presumably the lack of planarity leads to very weak coupling between the two ruthenium moieties. Extensive investigation of the photophysical properties supports the weak coupling. Perhaps the most compelling is the fact that excited state lifetimes of the dimers are longer than the monomers indicating that the ruthenium centers do not interact destructively.[40]

Given the above observations it appears that the dimers are well suited to an investigation of possibility that both centers can be oxidized or reduced photochemically and thus be converted into two electron donors or acceptors. Following is a description of initial investigations of quenching reactions design to yield two electron redox products. In particular the investigation will focus on the reactions of the excited state with $S_2O_8^{-2}$ and ascorbate. Reactions of $Ru(bpy)_3^{2+}$ and $Ru(phen)_3^{2+}$ with these reactants have been thoroughly investigated by previous workers. The quenching reaction with $S_2O_8^{2-}$ proceeds with an irreversible quantum yield of two strongly suggesting that the dimers will yield two electron oxidized products. Likewise ascorbate, based on previous work should yield a two electron reduced product and possibly hydrogen.

Chapter 2 Experimental

2.1 Materials

2-Methoxyethanol was purchased from Acros Organics. Triphenylphosphine (PPh_3), N,N-dimethylformamide (DMF), ammonium hexafluorophosphate (NH_4PF_6), the zinc dust, and 5-chloro-1,10-phenanthroline (Cl-phen) were all purchased from Alfa Aesar. Nickelous chloride hexahydrate ($NiCl_2 \cdot 6H_2O$) and potassium cyanide (KCN) were produced by J.T. Baker. Trimethylamine N-oxide (Me_3NO) was purchased from TCI. Ruthenium (III) chloride hydrate ($RuCl_3 \cdot XH_2O$) and 1,10-phenanthroline (phen) were purchased from Oakwood Chemical. Hydrochloric acid (HCl), diethyl ether, acetonitrile, methanol, and acetonitrile-d3 (CD_3CN) were produced by BDH. Formic acid (HCOOH) was produced by Mallinckrodt Chemicals. L-ascorbic acid (Vitamin C) sodium salt, ammonium persulfate ($(NH_4)_2S_2O_8$), ferrocene ($Fe(C_5H_5)_2$), and tetrabutylammonium hexafluorophosphate (NBu_4PF_6) were purchased from Sigma-Aldrich. Ammonium sulfate ($(NH_4)_2SO_4$) was purchased from Macron Chemicals.

2.2 Instrumentation and General Procedures

Infrared (IR) spectra were recorded with a Shimadzu IRAffinity-1S FTIR Spectroscopy equipped with a Quest ATR accessory with a diamond crystal puck. Samples were placed directly the sample holder and the empty chamber was scanned as the background. Spectra were collected in the range of 600 - 4000 cm^{-1} with 2 cm^{-1} resolution and 24 spectral scans averaged by the LabSolutionsIR operational software and then converted to Excel spreadsheets.

^{1}H-NMRwere recorded on a Bruker Avance 300 MHz Spectrometer.CD_3CN was used as solvent. NMR software TopSpin was used to analyze the spectra.

All ultraviolet-visible (UV/vis) absorption spectra were obtained using a Hewlett Packard 8452A Diode Array Spectrometer in conventional 1.0 cm quartz cells.

Fluorescence spectra were obtained with a Quanta Master^{TM} 300 Plus from Photon Technology International. The excitation wavelength was 450 nm and the emission spectra were recorded over the range of 480-800 nm at room temperature.

CH Instruments Electrochemical workstation was used for cyclic voltammetry with a three electrode system. The counter electrode was a platinum wire and the reference electrode was a silver wire. The working electrode was a platinum disc with a 1 mm diameter. The supporting electrolyte was 0.1 M NBu_4PF_6 in acetonitrile. Ferrocene was used as reference. All measurements were carried out at a scan rate of 100 mV/s.

Full structural analysis of the diphen was performed by Collin McMillen, Managing Director of the Molecular Structure Center in Clemson University by single crystal X-ray diffraction using a Rigaku AFC8 diffractometer with a sealed tube used to generate graphite monochromated Mo Kα (λ = 0.71073 Å) radiation. The diffractometer was equipped with a Mercury CCD detector. The diphen crystal was mounted on a glass fiber using epoxy glue, and data were collected at 100 K by omega scans over 480 diffraction images. Data processing was performed using the Crystal Clear software package. The space groups were determined from the systematic absences, and the structures were solved by direct methods and refined by least-squares techniques using the SHELXTL software suite.

2.3 Photochemical Procedures

Kinetics of Quenching Back-Reactions. Solutions containing $Ru(bpy)_3^{2+}$, $Ru(phen)_3^{2+}$ or dimer were excited with a PhaserR flash-lamp pumped dye laser with LD490 dye which

provided a 500 nsecpulse of 480 nm light. The probe beam was provided by a 100 watt tungsten lamp at right angle relative to the laser excitation. A shutter blocked the sample from irradiation by the probe prior to laser excitation. The probe beam was passed through a Kratos Schoeffel Instruments monochromator and the intensity monitored with a R446 photomultiplier. The signal was passed through a unity gain summing amplifier to allow subtraction of the steady state background signal. The transient absorbance changes were monitored by a LeCroy Model 6054 digital oscilloscope. The files were transferred to a PC for kinetic analysis.

In order to prevent possible changes in concentration due to the photoreaction, all the solutions were prepared and stored under darkroom conditions the same day as the experiment. However, no change of absorption was observed after storage of the solutions for a week with/without saturated nitrogen, which indicates the high stability of the ruthenium solutions. The ruthenium complexes concentrations employed in the quenching measurements varied from 22 to 60 μM, corresponding to an absorbance of 0.3-0.8 (ϵ 14000 M^{-1} cm^{-1}). The oxidative quenching measurements were performed with different concentrations of ammonium peroxodisulfate ($(NH_4)_2S_2O_8$) under air saturated at room temperature. The reductive quenching were performed with different concentrations of L-sodium ascorbic acid at pH =5 under nitrogen at room temperature.

2.4 Syntheses

2.4.1 5,5'-Bi-1,10-phenanthroline

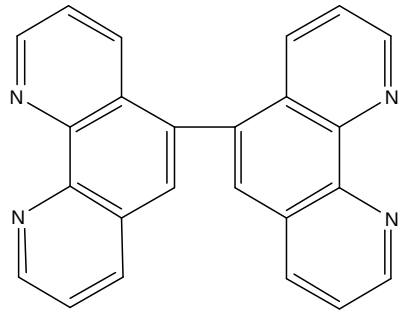

$NiCl_2 \cdot 6H_2O$ (0.304 g, 2.34 mmol) and PPh_3 (2.44 g, 9.30 mmol) were dissolved in 20 ml dry DMF in a 100 ml RBF and stirred at 50 °C under nitrogen for 1h. Unpurified zinc dust (0.27 g, 4.41 mmol) was added to the resulting blue solution. The solution was stirred at 50 °C under nitrogen until it was dark red. Cl-phen (0.496 g, 2.30 mmol) in 10 ml of DMF with nitrogen protection was added to the dark red solution. The solution was stirred at 50°C under nitrogen overnight until it was dark green. The resulting mixture was evaporated through the rotary evaporator to yield a dark green solid. Then the dark green solid was boiled in 80 ml of water for 2h. The mixture was cooled to room temperature and filtered. The yellow solution was precipitated with 10 ml of a saturated aqueous NH_4PF_6 solution. The precipitate was filtered by a medium porosity fritted funnel and then were suspended in a solution of KCN (1.50 g, 23.0 mmol) in 40 ml of a methanol and H_2O (19:1, v:v) and refluxed for 4 h. The resulting brown solution was cooled completely and filtered. The yellow solid was washed with H_2O and ether, and then dried in a desiccators (Yield: 49%).

2.4.2 Crystallization of 5,5'-Bi-1,10-phenanthroline

Diphen was dissolved in a minimum volume of hot CH_3CN in a RBF yielding a clear yellow solution. The solution was slowly cooled down to room temperature and allowed to stand undisturbed for 2 days. Yellow cubic crystals formed on the bottom.

2.4.3 $[(phen)_2Ru(diphen)Ru(phen)]PF_6$

$RuCl_3 \cdot XH_2O$ (2.02 g, 7.72 mmol) was dissolved in a 100 ml 1:1 (v:v) solution of concentrated HCl and HCOOH and refluxed for 24 h under nitrogen. The color of the solution changed from brown to yellow. The yellow solid was isolated through evaporation on a hotplate (Yield: 93%).

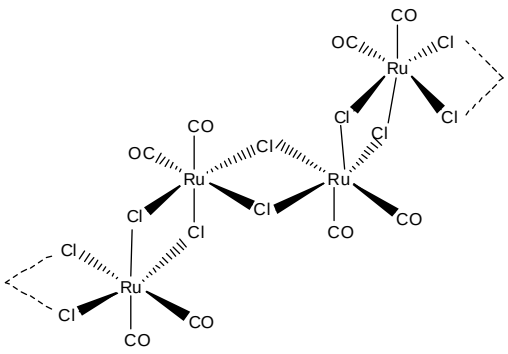

Diphen (0.462 g, 1.29 mmol) in 20 ml of hot 2-methoxyethanol was added to a solution of $[Ru(CO)_2Cl_2]_n$(1.47 g, 6.45 mmol) in 60 ml of hot 2-methoxyethanol in a 100 ml RBF and the resulting deep red solution was boiled for 7 min and cooled. The solution was filtered by a medium porosity fritted funnel, and the orange solid was dried in a desiccators (Yield: 37%).

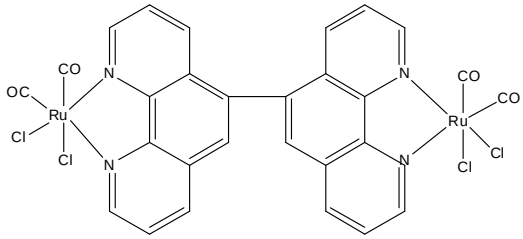

$[(phen)_2Ru(diphen)Ru(phen)_2](PF_6)_4$

$(CO)_2Cl_2Ru(diphen)Ru(CO)_2Cl_2$ (0.200 g, 0.246 mmol), phen (0.426 g, 2.36 mmol), and Me_3NO (0.187 g, 2.49 mmol) were suspended in 70 mL of nitrogen purged 2-methoxyethanol and refluxed for 2 h under nitrogen (dark brown). Me_3NO (0.05 g, 0.666 mmol) was added to the solution and continued refluxing for 1 h. The resulting solution was evaporated through the rotary. Then the oily solid was dissolved in 100 ml

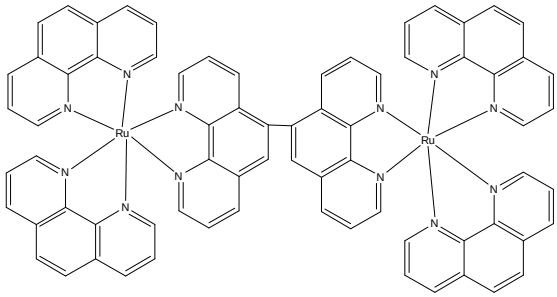

of water. Then the solution was precipitated with 10 ml of a saturated aqueous NH_4PF_6 solution. The precipitate was filtered by a medium porosity fritted funnel and then dried in a desiccator.

2.4.4 Crystallization of $[(phen)_2Ru(diphen)Ru(phen)](PF_6)_4$

Dissolved dimer in a minimum volume of CH_3CN in a RBF until formed a clear brown solution. Set the RBF aside undisturbed to evaporate CH_3CN. Brown needle-shaped crystals were precipitated on the bottom.

Chapter 3 Results

3.1 Synthesis and Basic Characterization of 5,5'-Bi-1,10-phenanthroline (diphen).

This investigation focused on photochemistry of $[(phen)_2Ru(diphen)Ru(phen)_2](PF_6)_4$and a comparison to corresponding monomeric complexes $[Ru(bpy)_3]^{2+}$ and $[Ru(phen)_3]^{2+}$. The nature of the investigations required synthetic procedures that provided reasonable yields and most importantly were free from contamination of the dimeric complex with $[Ru(phen)_3]^{2+}$ or $[Ru(phen)_2(diphen)]^{2+}$. $[Ru(bpy)_3](PF_6)_2$ and $[Ru(phen)_3](PF_6)_2$ have been thoroughly investigated and the synthesis of these complexes is well established.

The bridging ligand, diphen, was prepared using procedures previously reported[41] and later optimized by Puckett[40]. Briefly, diphen was prepared from 5-chloro-1,10-phenanthroline using a dichlorobis(triphenylphosphine)Ni(II), $Ni(PPh_3)_2Cl_2$, catalyst. Zinc metal is used to reduce $Ni(PPh_3)_2Cl_2$ in the present of triphenylphosphine in oxygen-free DMF to obtain a red-brown slurry of $Ni(PPh_3)_4$the catalyst for the reaction. The work-up procedures described in the previous chapter effectively eliminated triphenylphosphine from the product as indicated by NMR. Typical yields range from 30-50%.

$$Ni(PPh_3)_2Cl_2 + 2\ PPh_3 \xrightarrow{Zn\ /\ DMF\ /\ 50^oC\ /1\ h} Ni(PPh_3)_4$$

Scheme 3.1 Showing the homocoupling reaction used in the preparation of diphen

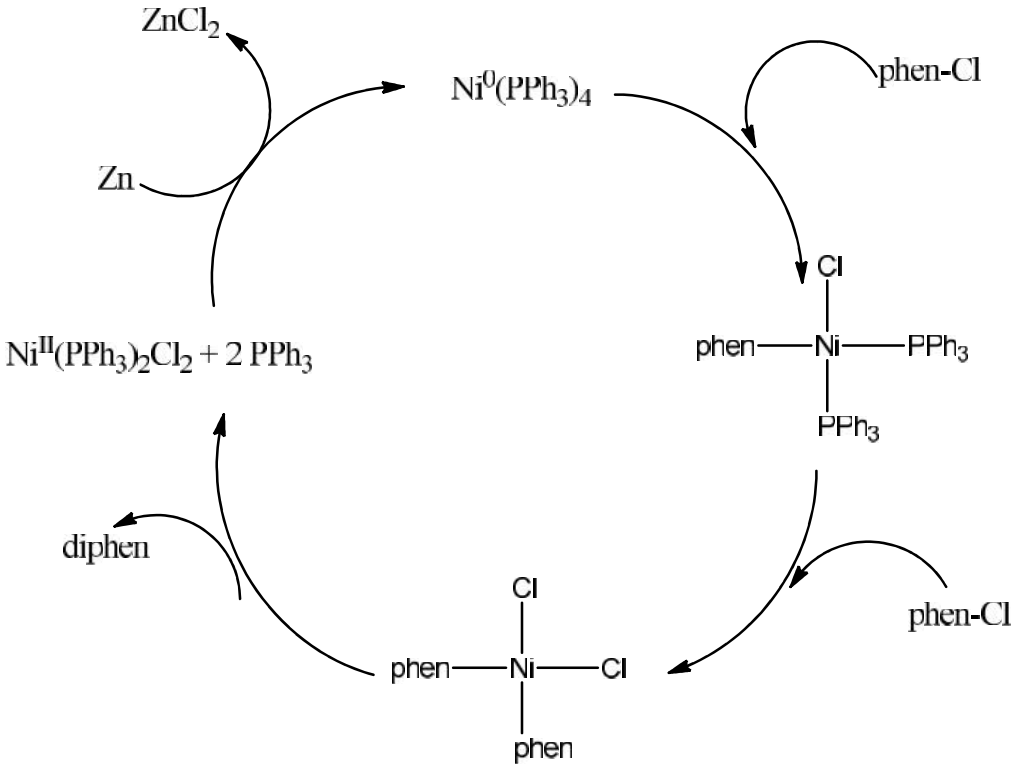
ZnCl2
Zn
Ni0(PPh3)4
phen-Cl
Cl
phen
Ni
PPh3
PPh3
NiII(PPh3)2Cl2 + 2 PPh3
diphen
Cl
phen
Ni
Cl
phen
phen-Cl

Diphen is readily soluble in polar organic solvents such as acetonitrile and was amenable to analysis by proton NMR. The ^{1}H-NMR of diphen in deuterated acetonitrile is shown in Figure 3.1. Interpretation of the spectrum is complicated by the fact that there are basically two chemically different phenanthroline moietiesthat are very similar. Comparison of the spectrum obtained with diphen to that of 1,10-phenanthroline shown in Figure 3.2 supports the presents of two spectrally dissimilar rings. The protons at the 4 and 7 positions are spectrally the most dissimilar. The close proximity of the rings of the adjacent phenanthroline shift the resonance of the 4 proton to 7.9 ppm whereas the resonance for the 7 proton remains at 8.5 ppm similar to that observed with the unsubstituted phenanthroline. The remaining assignments were based on the comparison to the spectrum 1,10-phenanthroline.The resonances centered at 9.15 ppm correspond to the protons at the 9 and 2 positions. Cross coupling in the COSEY spectrum of diphen shown in Figure 3.2 indicates that the resonance at 9.2 ppm corresponds to the proton at the 9 position (and the 9' position). The COSEY spectrum indicates that the resonances for the proton at the 3 position occurs at 7.5 ppm while the resonances for the proton at the 8 position appears at 7.8 ppm, again similar to the unsubstituted phenanthroline

Figure 3.1 ^{1}H NMR spectrum of diphen in CD_3CN

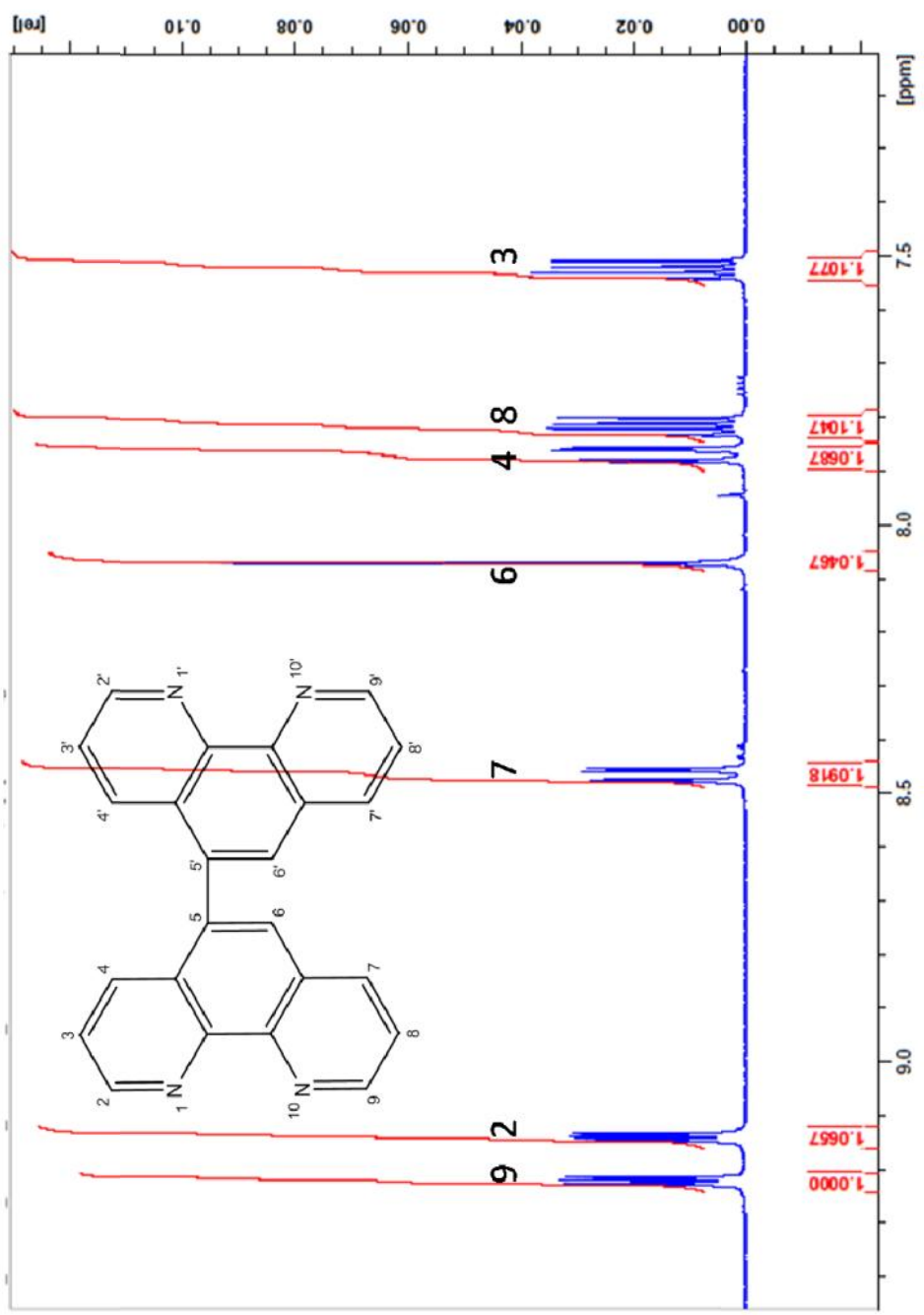
[rel]
0.00
0.02
0.04
0.06
0.08
0.10
[ppm]
7.5
8.0
8.5
9.0
3
8
4
6
7
2
9
1.1077
1.1047
1.0687
1.0467
1.0918
1.0657
1.0000

Figure 3.2 ^{1}H NMR spectrum of 1,10-phenanthroline in CD_3CN

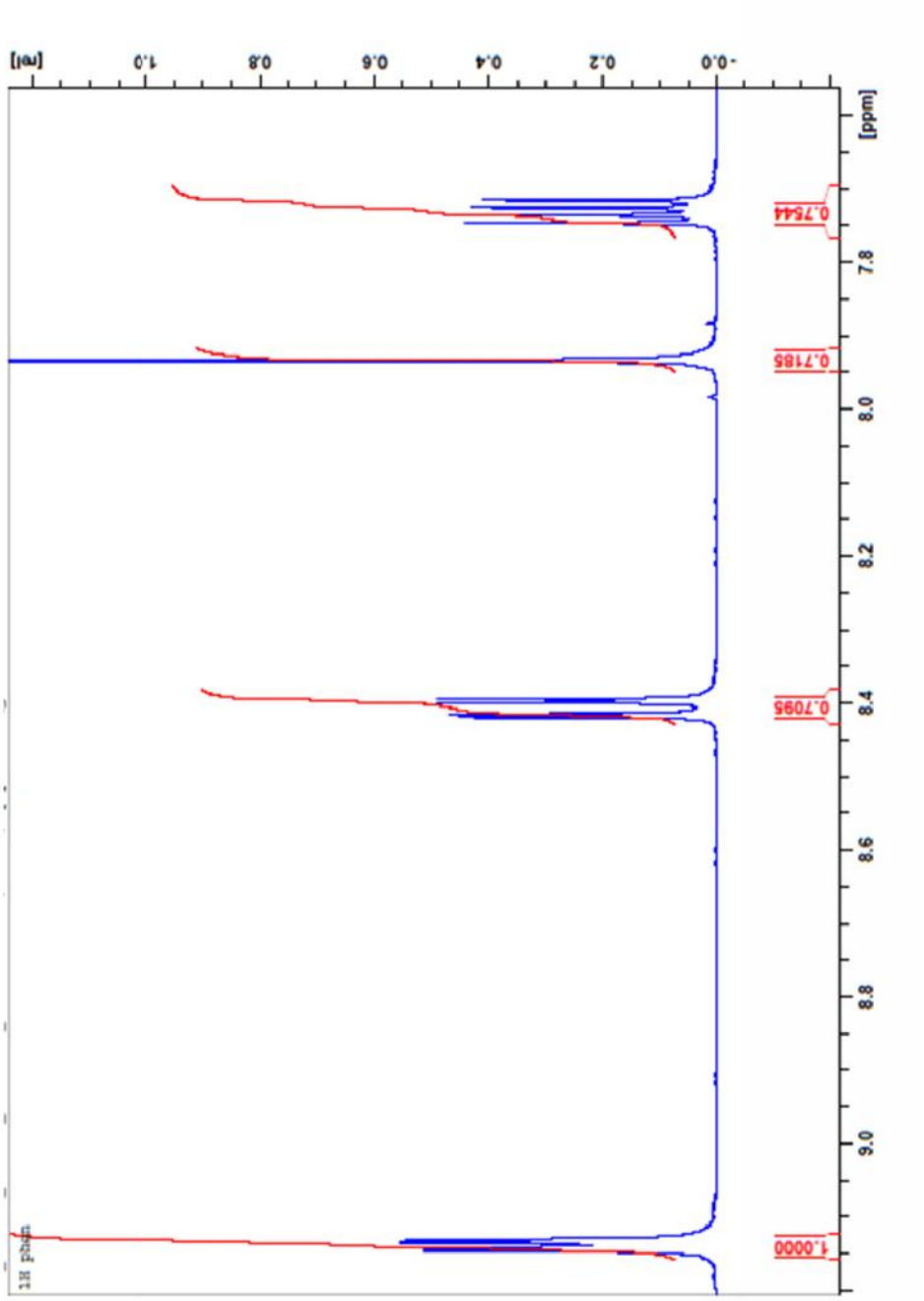
[rel]
0.0
0.2
0.4
0.6
0.8
1.0
[ppm]
7.8
8.0
8.2
8.4
8.6
8.8
9.0
0.7544
0.7185
0.7095
1.0000
1H phen

Figure 3.3 ^{1}H-^{1}H COSY spectrum of diphen in CD_3CN

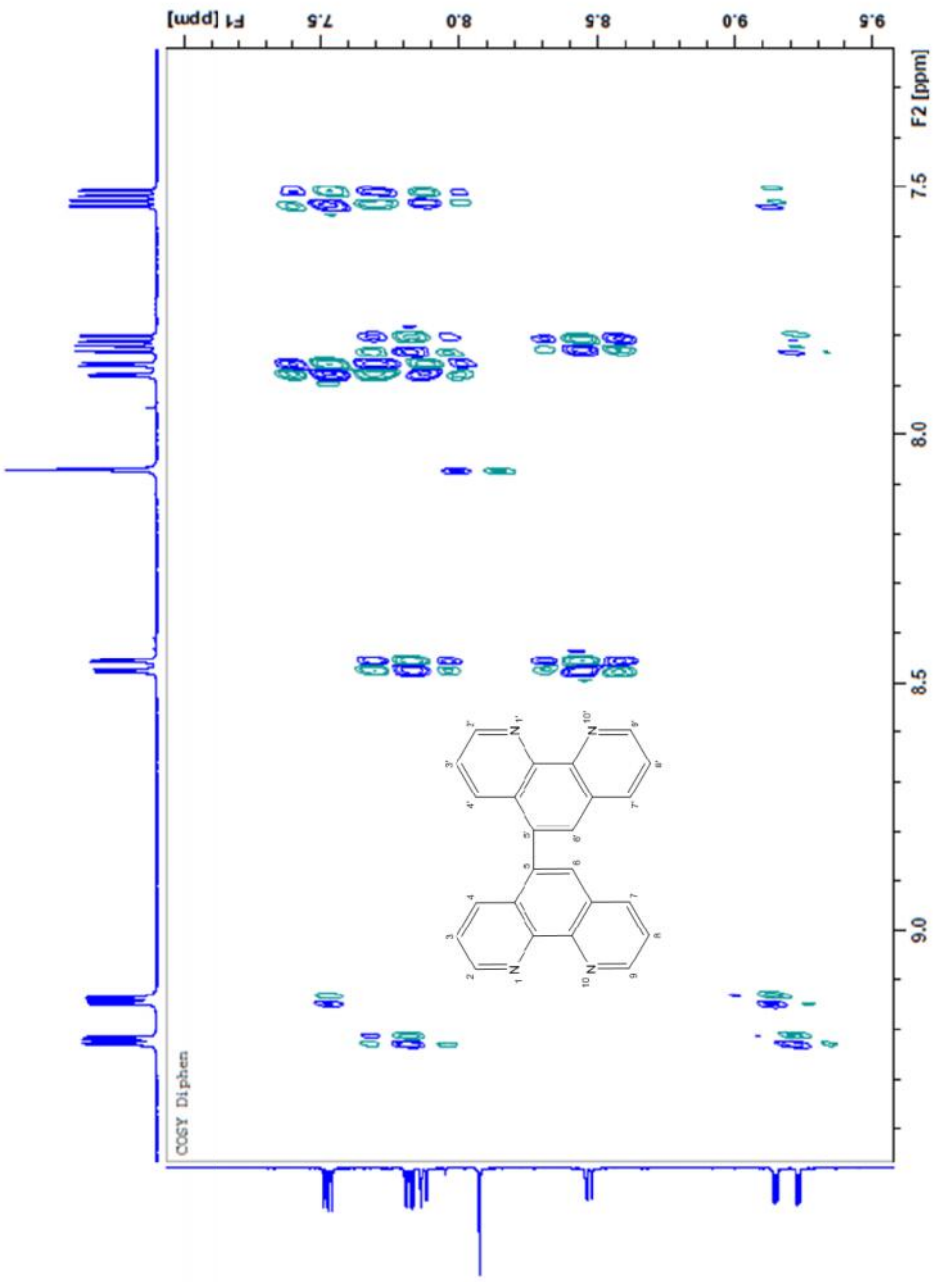
F1 [ppm]
9.5
9.0
8.5
8.0
7.5
F2 [ppm]
7.5
8.0
8.5
9.0
COSY Diphen

3.2 Synthesis and Basic Characterization of $[(phen)_2Ru(diphen)Ru(phen)_2](PF_6)_4$

$[(phen)_2Ru(diphen)Ru(phen)_2](PF_6)_4$was synthesize using a method similar to that used to prepare heteroleptic ruthenium polypyridyl complexes and later elaborated by Puckett[40] for the preparation of dimeric complexes. The following reactions summarize the chemistry

$$RuCl_3 + HCl + HCOOH \longrightarrow [Ru(CO)_2Cl_2]_n \qquad \text{eq 3.2.1}$$

$$[Ru(CO)_2Cl_2]_n + \frac{1}{2}\,n \text{ diphen} \xrightarrow{\text{2-methoxythanol}} n\,(CO)_2Cl_2Ru(diphen)Ru(CO)_2Cl_2 \qquad \text{eq 3.2.2}$$

$$(CO)_2Cl_2Ru(diphen)Ru(CO)_2Cl_2 + 2 \text{ phen} + 2\,Me_3NO \xrightarrow{\text{2-methoxythanol}}$$

$$[(phen)_2Ru(diphen)Ru(phen)_2]Cl_2 + 2Me_3N + 2CO_2 \qquad \text{eq 3.2.3}$$

$$[(phen)_2Ru(diphen)Ru(phen)_2]Cl_2 + 2NH_4PF_6 \xrightarrow{\text{2-methoxythanol}}$$

$$[(phen)_2Ru(diphen)Ru(phen)_2]PF_6 + 2\,NH_4Cl \qquad \text{eq 3.2.4}$$

The reaction described by eq 3.2.1 was originally developed by Aguirre[42] and has been used extensively as an entry point into the preparation of ruthenium polypyridyl complexes[43]. The diphen and phenanthroline were added stepwise in separate reactions. The final product was recovered by precipitation as indicated by eq. 3.2.4.

$[Ru(CO)_2Cl_2]_n$ is a common starting material used to prepare ruthenium polypyridine complexes. The synthesis is simple and proceeds in high yield of 90%. Although the structure of this complex is not well characterized, it is reproducible and it has characteristic carbonyl vibrational bands that are easily monitored by IR spectroscopy. The IR spectrum of $[Ru(CO)_2Cl_2]_n$ shows three absorption bands at 2011 cm^{-1}, 2063 $cm^{-1}$and 2139 cm^{-1}typical of metal complexes containing multiple carbonyl groups.

Reaction of $[Ru(CO)_2Cl_2]_n$ with diphen in 2-methoxyethanol results in the precipitation of a product in a few minutes at elevated temperatures consistent with the formulation $[(CO)_2Cl_2Ru(diphen)Ru(CO)_2Cl_2]$. The IR spectrum of the product reveals two absorption bands at 1978 cm^{-1} and 2054 cm^{-1}The number of bands and corresponding energies are typical of the asymmetric and symmetric stretching bands found in monomeric metal complex containing two carbonyl groups in the cis geometry.

$[(CO)_2Cl_2Ru(diphen)Ru(CO)_2Cl_2]$ was used without further purification. Addition of trimethylamine-N-oxide was used to convert the carbonyl groups to carbon dioxide which allowed the incorporation of four equivalents of 1,10-phenanthroline to produce $[(phen)_2Ru(diphen)Ru(phen)_2](PF_6)_4$. No absorption bands typical of metal carbonyls in the region around 2000 cm^{-1}were evident in the IR spectrum indicating the replacement of all of CO groups during the reaction.

Figure 3.4 Attenuated total reflectance IR spectrum of neat $[Ru(CO)_2Cl_2]_n$

Figure 3.5 Attenuated total reflectance IR spectrum of neat $[(CO)_2Cl_2Ru(diphen)Ru(CO)_2Cl_2]$

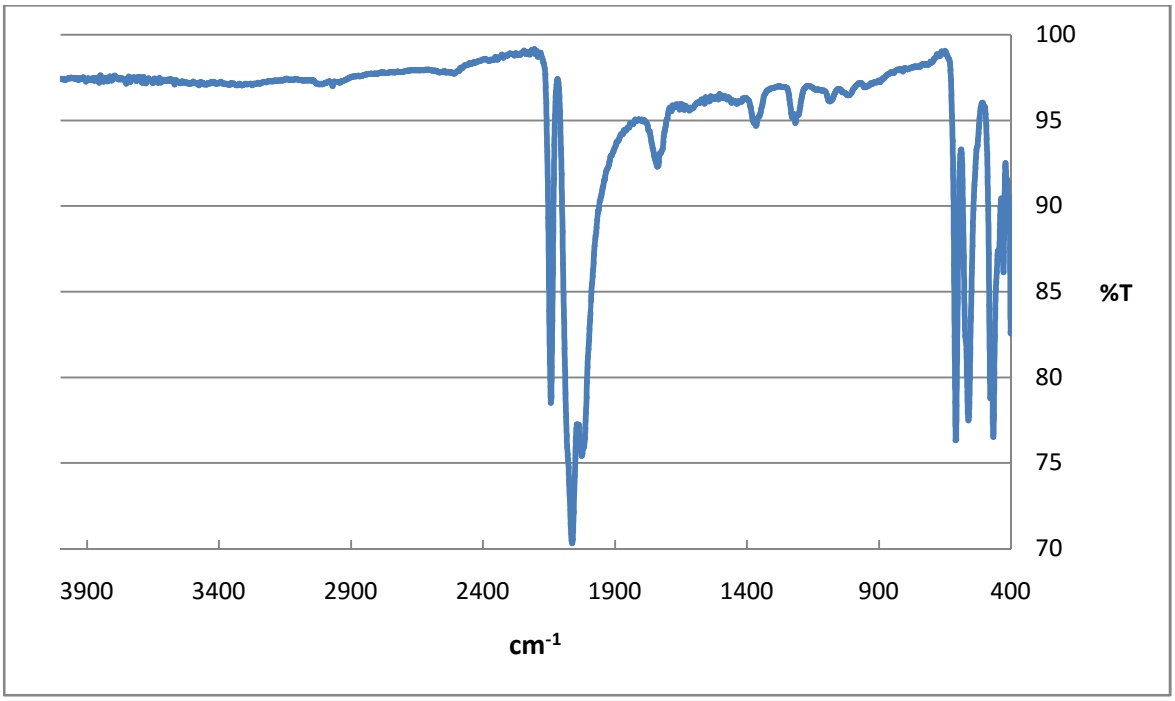
100
95
90
85
%T
80
75
70
3900
3400
2900
2400
1900
1400
900
400
cm-1

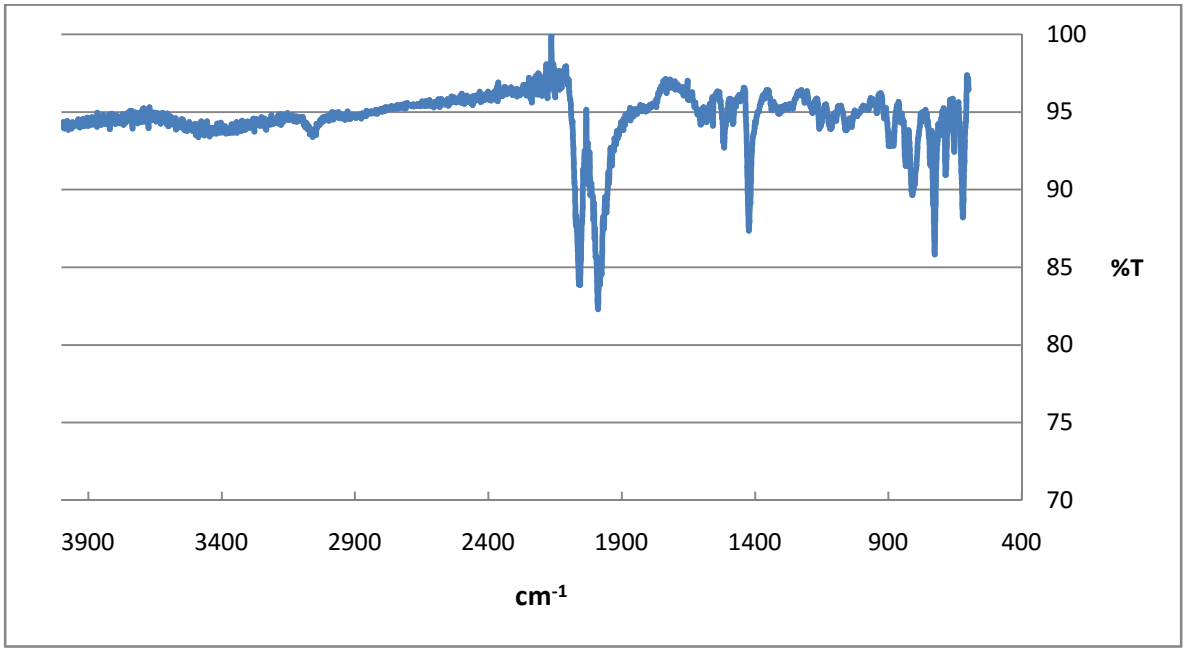
100
95
90
85
%T
80
75
70
3900
3400
2900
2400
1900
1400
900
400
cm-1

Figure 3.6 Attenuated total reflectance IR spectrum of neat $[(phen)_2Ru(diphen)Ru(phen)_2](PF_6)_4$

Figure 3.7 Attenuated total reflectance IR spectrum of neat 1,10-phenanthroline

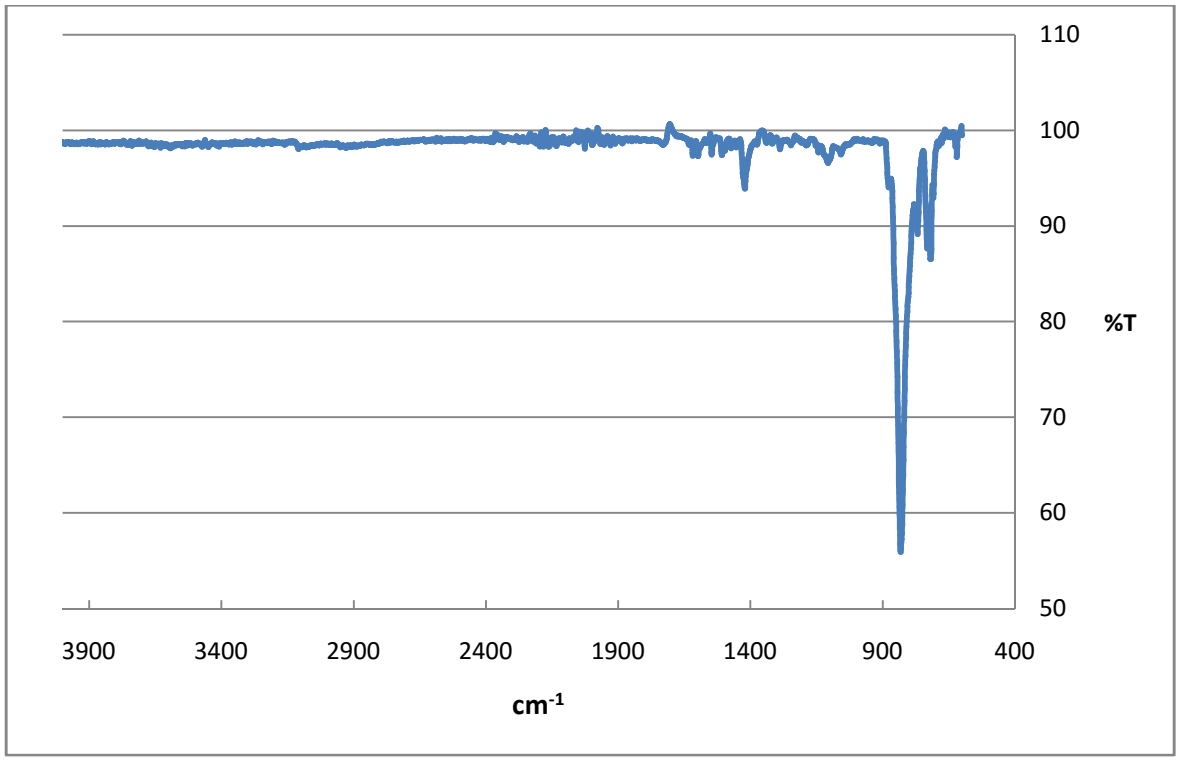
110
100
90
80
70
60
50
%T
3900
3400
2900
2400
1900
1400
900
400
cm-1

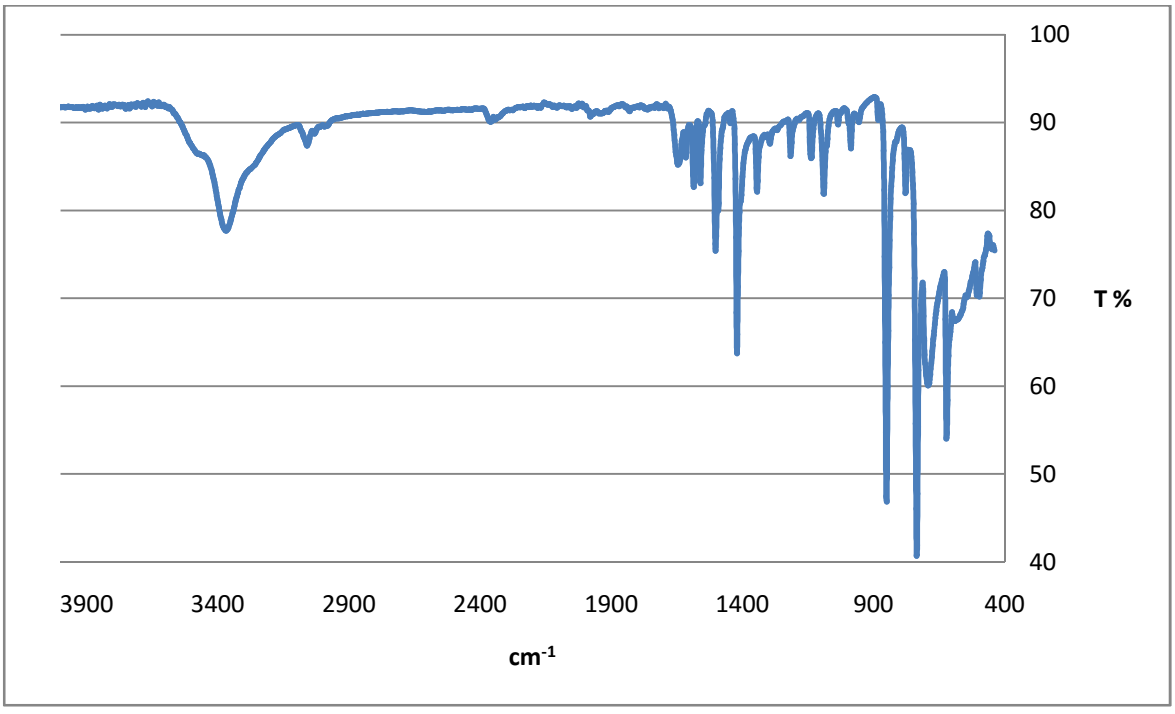
100
90
80
70
60
50
40
T %
3900
3400
2900
2400
1900
1400
900
400
cm-1

The ^{1}H-NMR of dimer in deuterated acetonitrile is shown in Figure 3.8. Interpretation of the spectrum is challenging in light of the fact that there are many similar abut not identical heterocyclic rings. The spectrum shown in Figure 3.8 lacks the resolution to reveal the dissimilarities. However, the general features are consistent with the target complex. Comparison of the spectrum obtained with dimer to that of diphen clearly illustrates the structure is highly symmetric. The resonances centered at 9.1 ppm correspond to the protons at the 9 and 2 positions. The protons at the 4 and 7positions are spectrally closer than it shows in diphen. The protons at 5 and 6 positions are identical. The resonances for the 3 and 8 protons occur at 7.8 ppm, again similar to the unsubstituted phenanthroline. The peaks indicated with X are impurities. Integration of the peaks is consistent with the target structure.

The UV-Visible absorption spectrum of the product and the corresponding monomer $[Ru(phen)_3]^{2+}$ are shown in Figures 3.9 and 3.10 respectively. Comparison of the two spectra indicates that spectroscopically the two complexes are nearly identical showing a λ_{max} value of 448nm.

Figure 3.8 ^{1}H NMR spectrum of $[(phen)_2Ru(diphen)Ru(phen)_2](PF_6)_4$ in CD_3CN

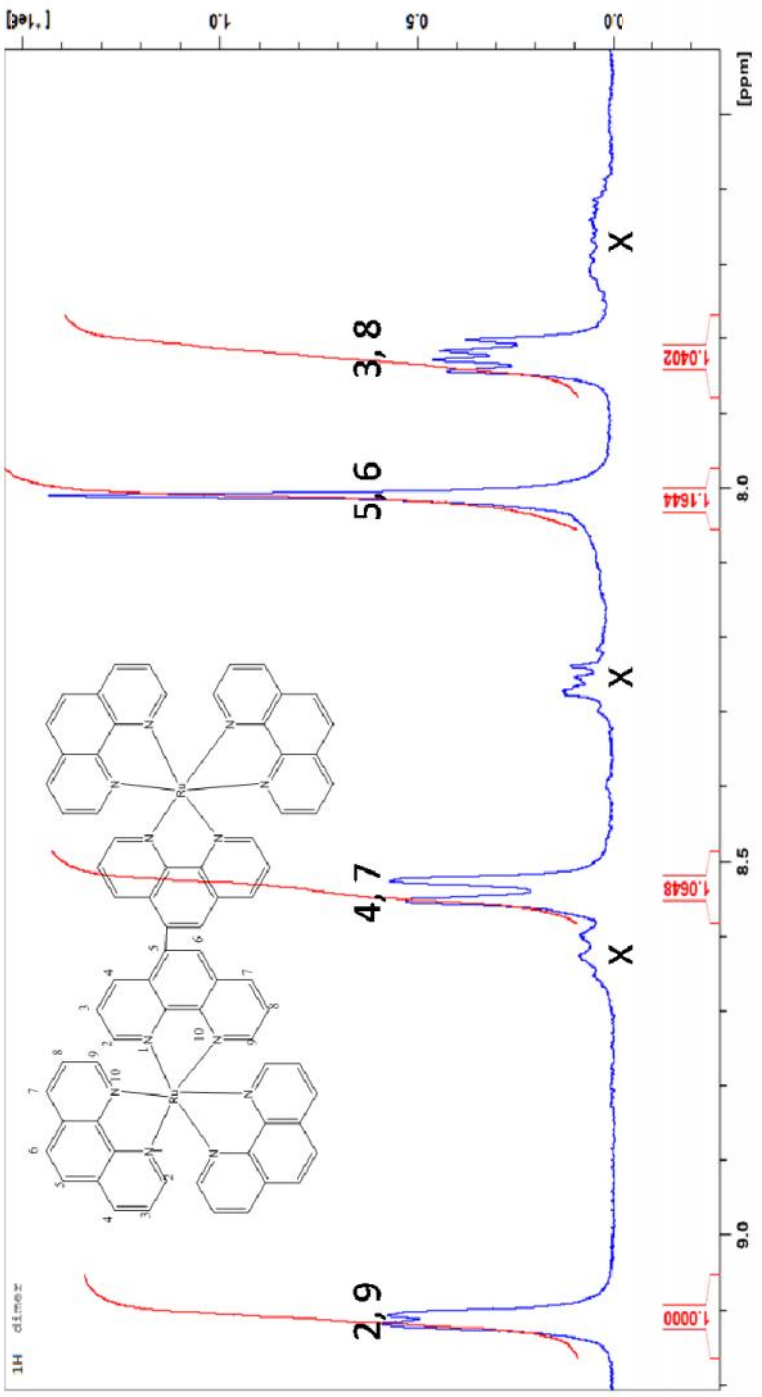
1H dimer
2, 9
4, 7
5, 6
3, 8
X
X
X
1.0000
1.0648
1.1644
1.0402
9.0
8.5
8.0
[ppm]

Figure 3.9 UV-Vis spectrum of $[(phen)_2Ru(diphen)Ru(phen)_2](PF_6)_4$ in acetonitrile

Figure 3.10 UV-Vis spectrum of $Ru(phen)_3Cl_2$ in 0.2 M $(NH_4)_2SO_4$

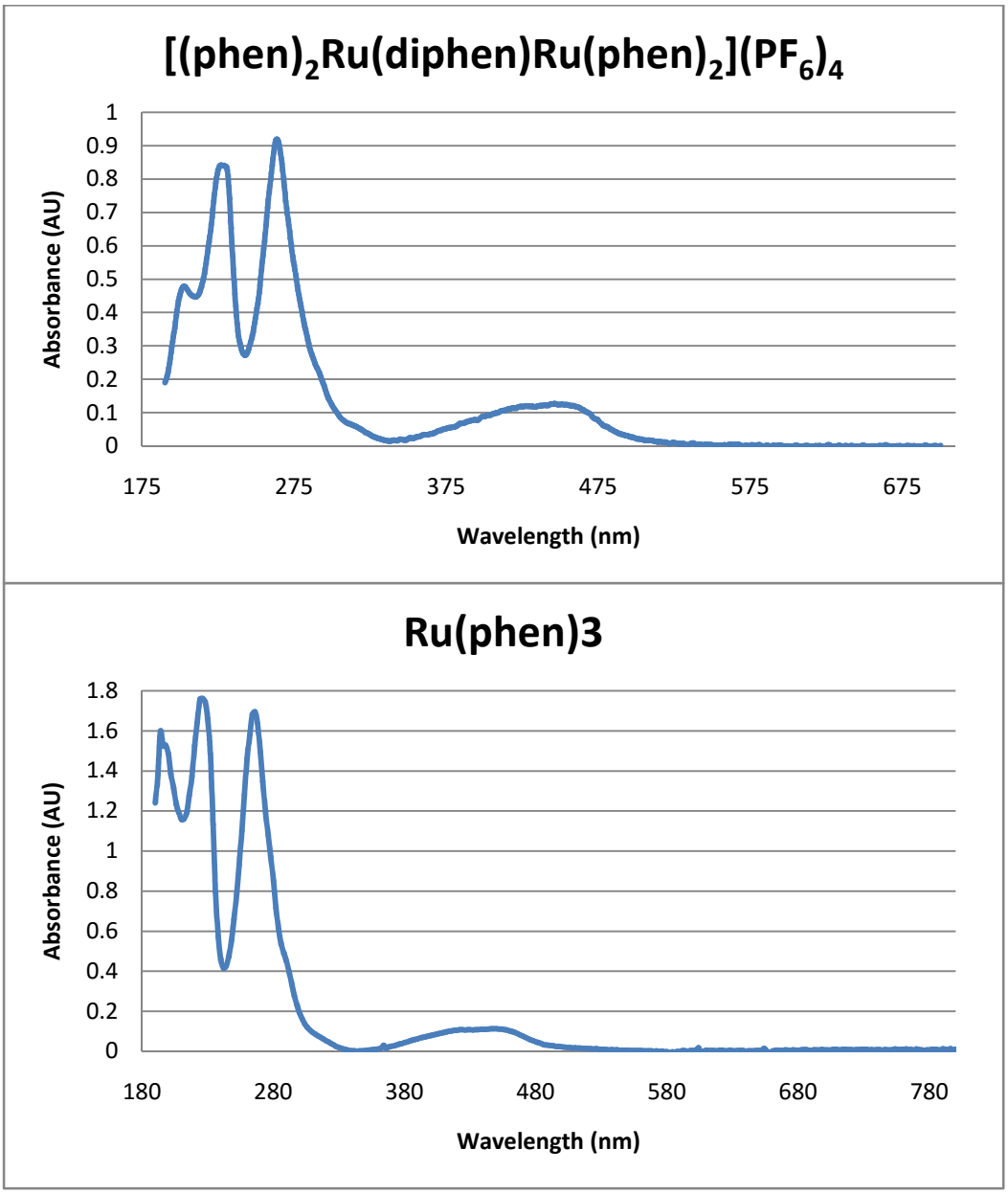
[(phen)2Ru(diphen)Ru(phen)2](PF6)4
Absorbance (AU)
1
0.9
0.8
0.7
0.6
0.5
0.4
0.3
0.2
0.1
0
175
275
375
475
575
675
Wavelength (nm)
Ru(phen)3
Absorbance (AU)
1.8
1.6
1.4
1.2
1
0.8
0.6
0.4
0.2
0
180
280
380
480
580
680
780
Wavelength (nm)

3.3 Structure of 5,5'-Bi-1,10-Phenanthroline

Small golden cubic crystals of diphen were obtained by slow evaporation of an acetonitrile solution. Full structure analysis of diphen crystals was performed by single crystal X-ray diffraction. Plots of the structure of diphen single molecule are shown in Figure 4.1. Selected bond lengths and angles are reported in Table 3.1-3.3.

3.4 Electrochemical studies (CV)

$$E_{1/2} = \frac{1}{2}(1.015\ V + 0.973\ V) = 0.994\ V$$

The redox potential for $[(phen)_2Ru(diphen)Ru(phen)_2](PF_6)_4$ is 0.994 V vs Ag/AgCl, which is similar with $Ru(phen)_3^{2+}$ with a redox potential of 0.858V vs Ag/AgCl.

$[(phen)_2Ru(diphen)Ru(phen)_2](PF_6)_4$ exhibits three consecutive cathodic couples (ligand-based reductions) at -0.343, -0.807, -1.095 V vs Ag/AgCl.

Table 3.1 Sample and crystal data for diphen**.**

Chemical formula	$C_{26}H_{17}N_5$	
Formula weight	399.45 g/mol	
Temperature	100(2) K	
Wavelength	1.54178 Å	
Crystal size	0.151 x 0.188 x 0.202 mm	
Crystal system	monoclinic	
Space group	C 1 2/c 1	
Unit cell dimensions	a = 16.7253(7) Å	α = 90°
	b = 11.2482(5) Å	β = 120.6180(10)°
	c = 11.5844(5) Å	γ = 90°
Volume	1875.52(14) $Å^3$	
Z	4	
Density (calculated)	1.415 g/cm^3	
Absorption coefficient	0.685 mm^{-1}	
F(000)	832	

Table 3.2 Bond lengths (Å) for diphen.

N1-C1	1.325(2)	N1-C5	1.361(2)
N2-C10	1.321(2)	N2-C6	1.357(2)
C12-C11	1.357(2)	C12-C7	1.451(2)
C12-C12	1.494(3)	C6-C7	1.412(2)
C6-C5	1.453(2)	C4-C5	1.409(3)
C4-C3	1.412(2)	C4-C11	1.435(2)
C3-C2	1.369(3)	C3-H3	0.95
C11-H11	0.95	C7-C8	1.412(3)
C8-C9	1.371(3)	C8-H8	0.95
C1-C2	1.403(3)	C1-H1	0.95
C9-C10	1.405(3)	C9-H9	0.95
C10-H10	0.95	C2-H2	0.95
C13A-C13A	1.67037(4)	C13A-H13A	0.98
C13A-H13B	0.98	C13A-H13C	0.98
N14-C13A	1.11703(4)	N13-C14	1.11719(3)
C14-C15	1.15875(5)	C15-H15A	0.98
C15-H15B	0.98	C15-H15C	0.98

Table 3.3 Bond angles (°) for diphen

C1-N1-C5	117.25(16)	C10-N2-C6	117.99(16)
C11-C12-C7	119.79(16)	C11-C12-C12	120.56(13)
C7-C12-C12	119.65(13)	N2-C6-C7	122.81(16)
N2-C6-C5	117.99(16)	C7-C6-C5	119.20(16)
C5-C4-C3	117.89(17)	C5-C4-C11	120.01(16)
C3-C4-C11	122.04(16)	C2-C3-C4	118.68(17)
C2-C3-H3	120.7	C4-C3-H3	120.7
C12-C11-C4	121.51(16)	C12-C11-H11	119.2
C4-C11-H11	119.2	C6-C7-C8	117.06(16)
C6-C7-C12	120.17(16)	C8-C7-C12	122.77(17)
C9-C8-C7	120.02(18)	C9-C8-H8	120.0
C7-C8-H8	120.0	N1-C5-C4	122.99(16)
N1-C5-C6	117.83(16)	C4-C5-C6	119.16(16)
N1-C1-C2	123.78(17)	N1-C1-H1	118.1
C2-C1-H1	118.1	C8-C9-C10	118.23(17)
C8-C9-H9	120.9	C10-C9-H9	120.9
N2-C10-C9	123.86(17)	N2-C10-H10	118.1
C9-C10-H10	118.1	C3-C2-C1	119.39(17)
C3-C2-H2	120.3	C1-C2-H2	120.3
C13A-C13A-H13A	109.5	C13A-C13A-H13B	109.5
H13A-C13A-H13B	109.5	C13A-C13A-H13C	109.5
H13A-C13A-H13C	109.5	H13B-C13A-H13C	109.5
N13-C14-C15	168.7410(10)	C14-C15-H15A	109.5
C14-C15-H15B	109.5	H15A-C15-H15B	109.5
C14-C15-H15C	109.5	H15A-C15-H15C	109.5
H15B-C15-H15C	109.5		

Figure 3.11 Cyclic Votammogram of $[(phen)_2Ru(diphen)Ru(phen)_2](PF_6)_4$in 0.1M $TBAPF_6$ in acetonitrile versus Ag/AgCl

Figure 3.12 Cyclic Voltammogram of $[(phen)_2Ru(diphen)Ru(phen)_2](PF_6)_4$ under nitrogen in 0.1M TBAPF6 in acetonitrile.

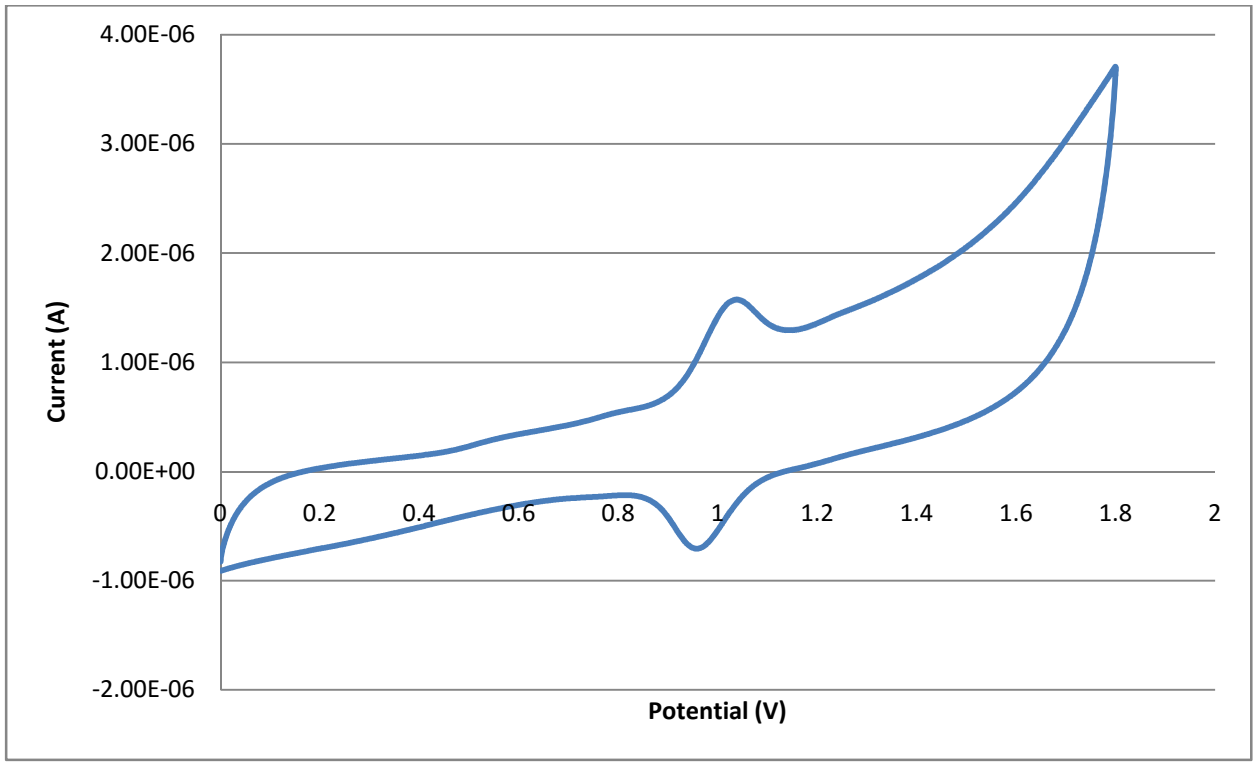
4.00E-06
3.00E-06
2.00E-06
1.00E-06
0.00E+00
-1.00E-06
-2.00E-06
Current (A)
0
0.2
0.4
0.6
0.8
1
1.2
1.4
1.6
1.8
2
Potential (V)

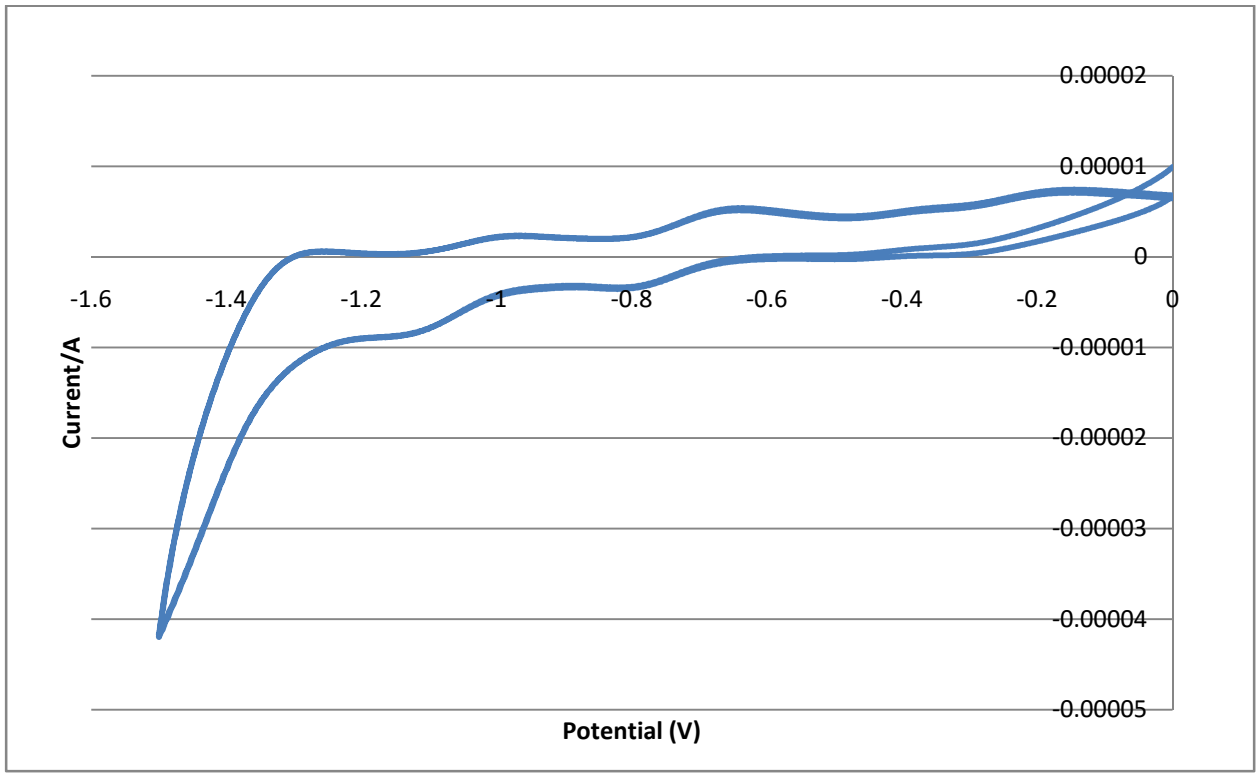
0.00002
0.00001
0
-0.00001
-0.00002
-0.00003
-0.00004
-0.00005
Current/A
-1.6
-1.4
-1.2
-1
-0.8
-0.6
-0.4
-0.2
0
Potential (V)

3.5 Oxidative Quenching of Ru(II) Dimer and Monomers by Peroxydisulfate

The quenching reactions of $Ru(bpy)_3^{2+}$, $Ru(phen)_3^{2+}$ and the dimer in aqueous solutions by $S_2O_8^{2-}$ were investigated using traditional Stern-Volmer techniques steady-state irradiation and laser flash photolysis. The monomeric complexes have been previously investigated in detail and were used for comparison. The focus of the laser experiments was twofold; monitor the rate of the back-reaction and measure, by comparison, the quantum yield for the quenching reaction. The steady-state irradiation experiments were also done to provide information about the quantum yield for product formation.

In the fluorescence measurements, the ruthenium complexes concentrations are enough to provide an absorbance of around 0.8, and the concentrations of $S_2O_8^{2-}$ were varied from 0 to $3.0x10^{-4}$ mol L^{-1}. When excited with a wavelength of 450 nm, the ruthenium complexes have a strong fluorescence emission peaked at 605 nm. The addition of $S_2O_8^{2-}$ caused a gradual decrease in the fluorescence intensity of ruthenium complexes and the emission had a red-shift for the dimer and $[Ru(phen)_3]^{2+}$. This suggested that the microenvironment around the dimer and $[Ru(phen)_3]^{2+}$was changed after the addition of $S_2O_8^{2-}$.

Stern-Volmer plots for $S_2O_8^{2-}$ quenching of ruthenium complexes fluorescence are shown in Figure 3.17. The possible quenching reactions were analyzed by the Stern-Volmer equation:

$$\frac{I_0}{I} = 1 + k_q \tau_0 [Q] = 1 + K_{sv}[Q]$$

Where I_0 and I are the steady-state fluorescence intensities in the absence and presence of $S_2O_8^{2-}$ quencher, respectively, k_q the bimolecular quenching rate constant, τ_0 the life time of fluorescence in absence of $S_2O_8^{2-}$, K_{sv} the Stern-volmer quenching constant, and [Q] the

concentration of $S_2O_8^{2-}$. Hence the above equation could be applied to determine k_q by linear regression of a plot of I_0/I against. The result shows that the quenching constant (Figure 3.17 and Table 3.1), k_q, for the dimer is higher than $[Ru(phen)_3]^{2+}$.

A representative absorption transient showing the formation of Ru(III) from ruthenium(II) complexes are shown in Figure 3.17 and 3.18. Absorbance changes $\Delta A = 0.0946$ for dimer, which is about two times as $\Delta A = 0.0474$ for $Ru(phen)_3^{2+}$. Absorbance changes ΔA are 0.1410 and 0.0988 for dimer and $Ru(bpy)_3^{2+}$, respectively. The slow down curves showed in the monomers $Ru(phen)_3^{2+}$ and $Ru(bpy)_3^{2+}$ show that the formation of Ru(III) is slower than form dimer.

A 300 watt, 120 volt bulb "sunlamp" with no filtering was also used for photochemical reactions. The photochemical reaction of the dimer and $S_2O_8^{2-}$ was monitored via UV-vis spectroscopy. The spectra can be seen in Figure 3.20. Figure 3.19 for $Ru(phen)_3^{2+}$ is used as a comparison. The peak at 448 nm, which is correlates to the Ru(II) concentration, decreases over time. This is the expected result of a quench reaction where $Ru(II)^*$ is oxidized by $S_2O_8^{2-}$ to Ru(III). Absorbance changes ΔA at 30 s are 0.5837 and 0.05145 for dimer and $Ru(phen)_3^{2+}$, respectively. With the time consuming, the absorbance changes of $Ru(phen)_3^{2+}$ become much smaller, where as the dimer almost maintain the same, which means the dimer excited state is more stable.

Oxidation reaction of the dimer was performed with fresh produced chlorine, and the product was detected with UV-vis spectroscopy showed in Figure 3.21. Figure 3.22 for $Ru(bpy)_3^{2+}$ is used as a comparison. A new peak shows at 622 nm only for the dimer, which means different product is being formed from $Ru(bpy)_3^{2+}$.

A representative absorption transient showing the rapid formation of Ru(I) and the subsequent slow back reaction that returns the system to the initial state is shown in Figure 3.27. Absorbance changes ΔA are 0.0231, 0.0289 and 0.0199 for $Ru(bpy)_3^{2+}$, $Ru(phen)_3^{2+}$ and dimer, respectively.

Table 3.4 Stern-Volmer quenching constants for the ruthenium complexes with $S_2O_8^{2-}$

pH	Ruthenium complexes	τ_0 (ns)	K_{sv} ($\times 10^3$ M^{-1})	k_q ($\times 10^9$ $M^{-1}s^{-1}$)
4	$[(phen)_2Ru(diphen)Ru(phen)_2]^{2+}$	1470	9.719	6.612
	$[Ru(phen)_3]^{2+}$	1000	2.236	2.236
	$[Ru(bpy)_3]^{2+}$	590	7.050	11.95

Figure 3.13 Effect of [$S_2O_8^{2-}$] on the emission intensity of the dimer in 0.2 M $(NH_4)_2SO_4$

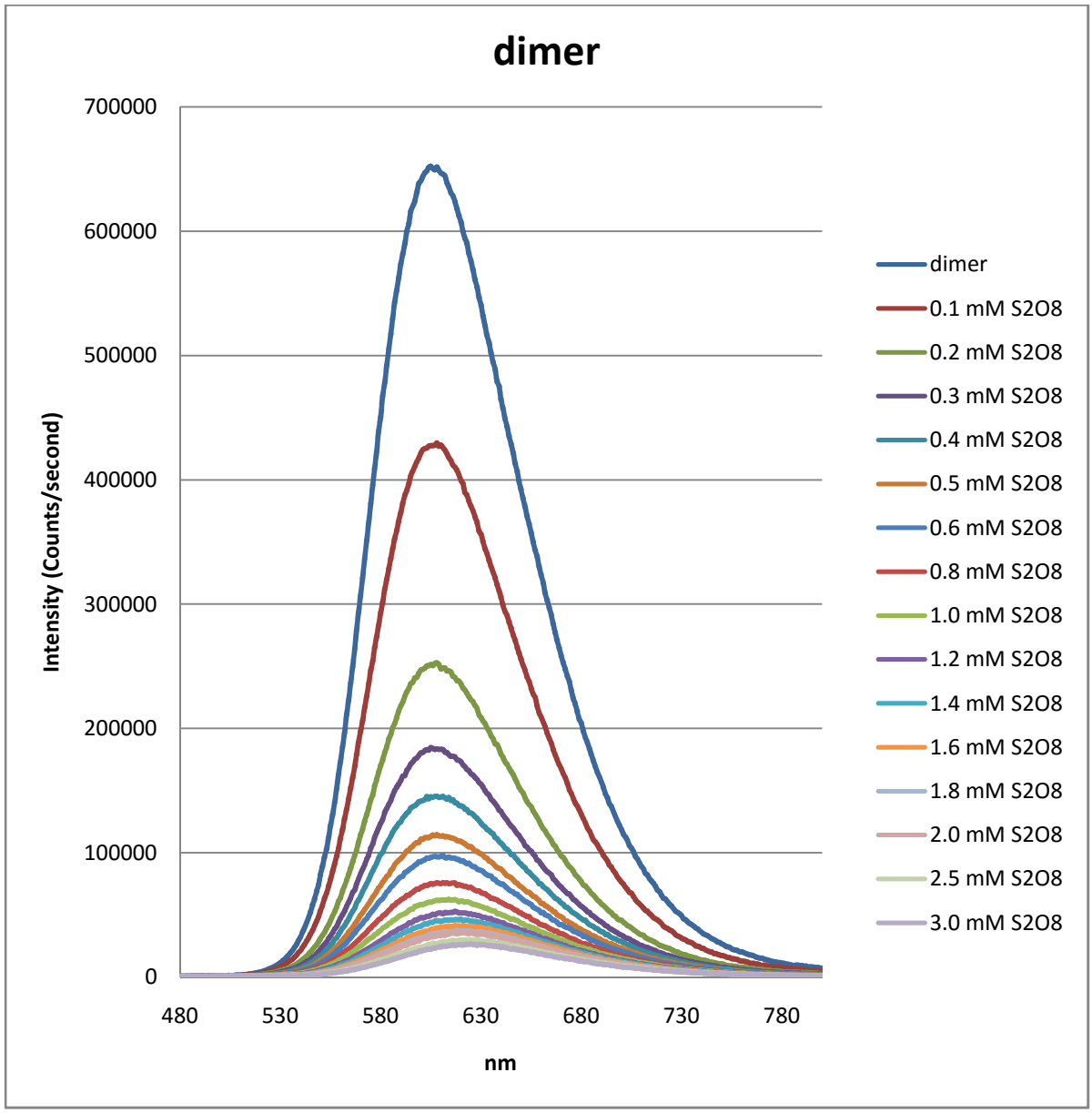
dimer
700000
600000
500000
400000
300000
200000
100000
0
Intensity (Counts/second)
480
530
580
630
680
730
780
nm
dimer
0.1 mM S2O8
0.2 mM S2O8
0.3 mM S2O8
0.4 mM S2O8
0.5 mM S2O8
0.6 mM S2O8
0.8 mM S2O8
1.0 mM S2O8
1.2 mM S2O8
1.4 mM S2O8
1.6 mM S2O8
1.8 mM S2O8
2.0 mM S2O8
2.5 mM S2O8
3.0 mM S2O8

Figure 3.14 Effect of [$S_2O_8^{2-}$] on the emission intensity of $Ru(phen)_3^{2+}$ in 0.2 M $(NH_4)_2SO_4$

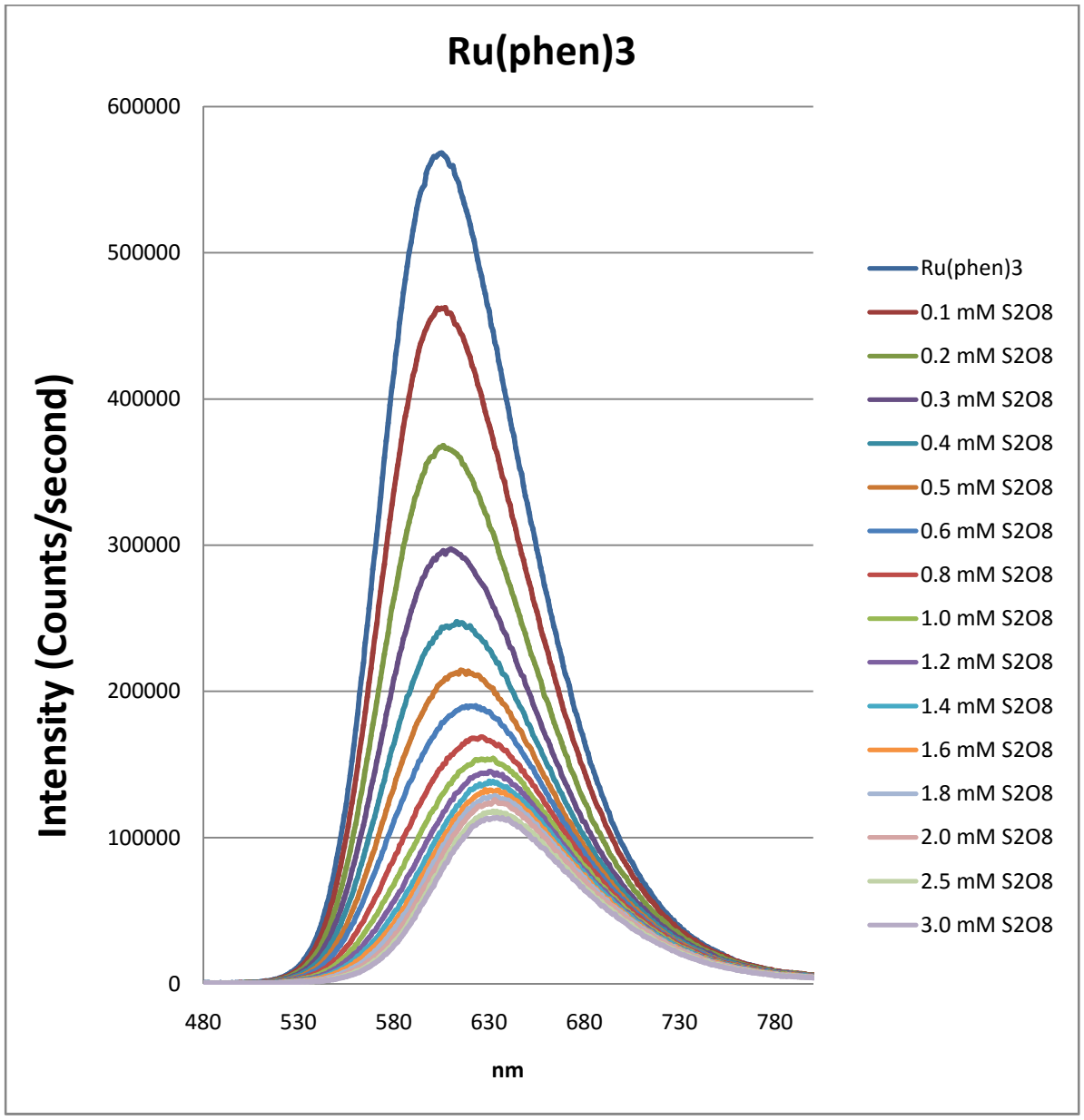
Ru(phen)3
Intensity (Counts/second)
600000
500000
400000
300000
200000
100000
0
480
530
580
630
680
730
780
nm
Ru(phen)3
0.1 mM S2O8
0.2 mM S2O8
0.3 mM S2O8
0.4 mM S2O8
0.5 mM S2O8
0.6 mM S2O8
0.8 mM S2O8
1.0 mM S2O8
1.2 mM S2O8
1.4 mM S2O8
1.6 mM S2O8
1.8 mM S2O8
2.0 mM S2O8
2.5 mM S2O8
3.0 mM S2O8

Figure 3.15 Effect of [$S_2O_8^{2-}$] on the emission intensity of $Ru(bpy)_3^{2+}$ in 0.2 M $(NH_4)_2SO_4$.

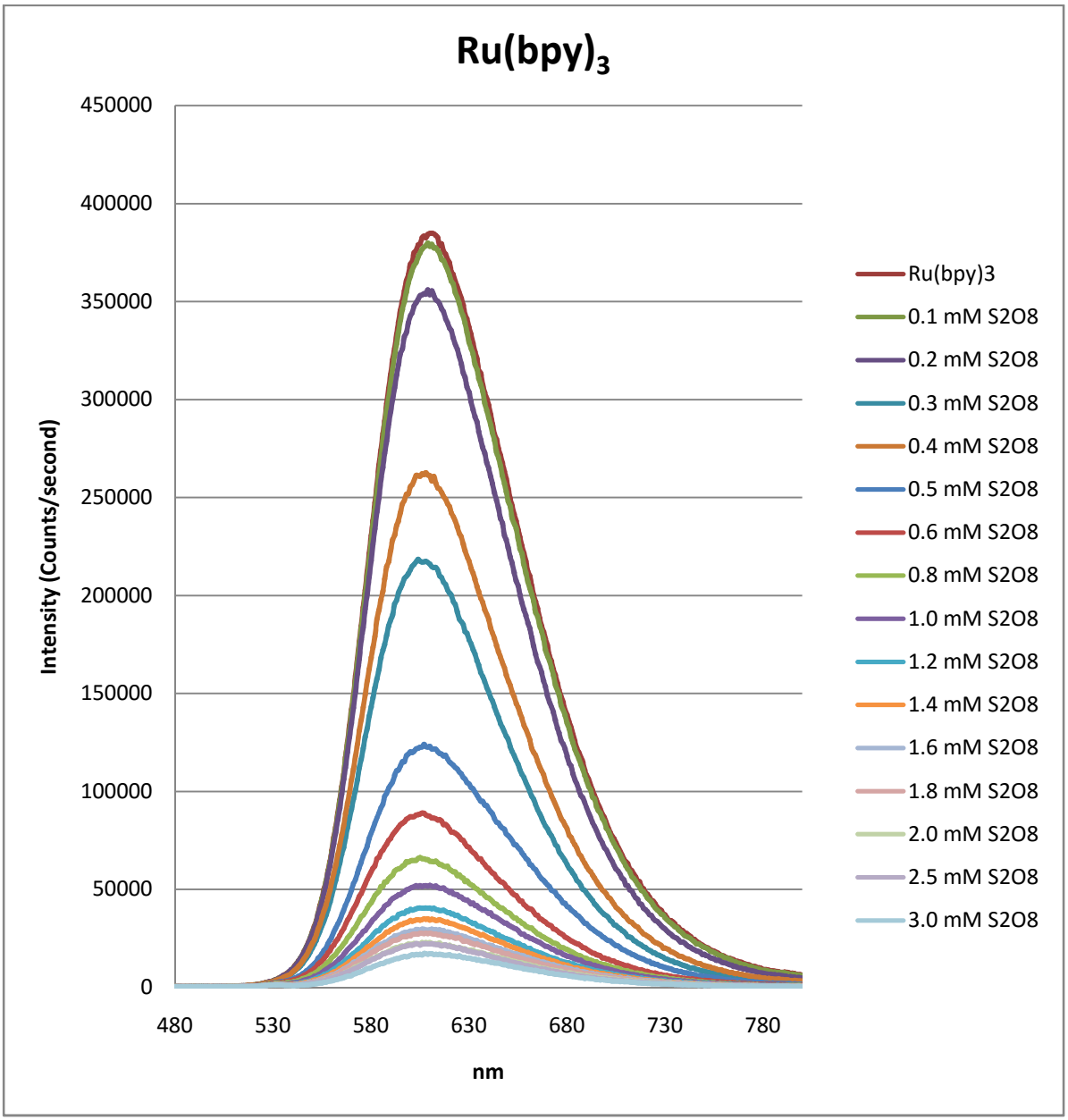
Ru(bpy)3
450000
400000
350000
300000
250000
200000
150000
100000
50000
0
Intensity (Counts/second)
480
530
580
630
680
730
780
nm
Ru(bpy)3
0.1 mM S2O8
0.2 mM S2O8
0.3 mM S2O8
0.4 mM S2O8
0.5 mM S2O8
0.6 mM S2O8
0.8 mM S2O8
1.0 mM S2O8
1.2 mM S2O8
1.4 mM S2O8
1.6 mM S2O8
1.8 mM S2O8
2.0 mM S2O8
2.5 mM S2O8
3.0 mM S2O8

Figure 3.16 Plots of the relative emission intensities of $Ru(bpy)_3^{2+}$, $Ru(phen)_3^{2+}$ and the dimer versus the $[S_2O_8^{2-}]$ concentration. The solid lines and the associated equations were obtained using linear least squares and are the "best" fits.

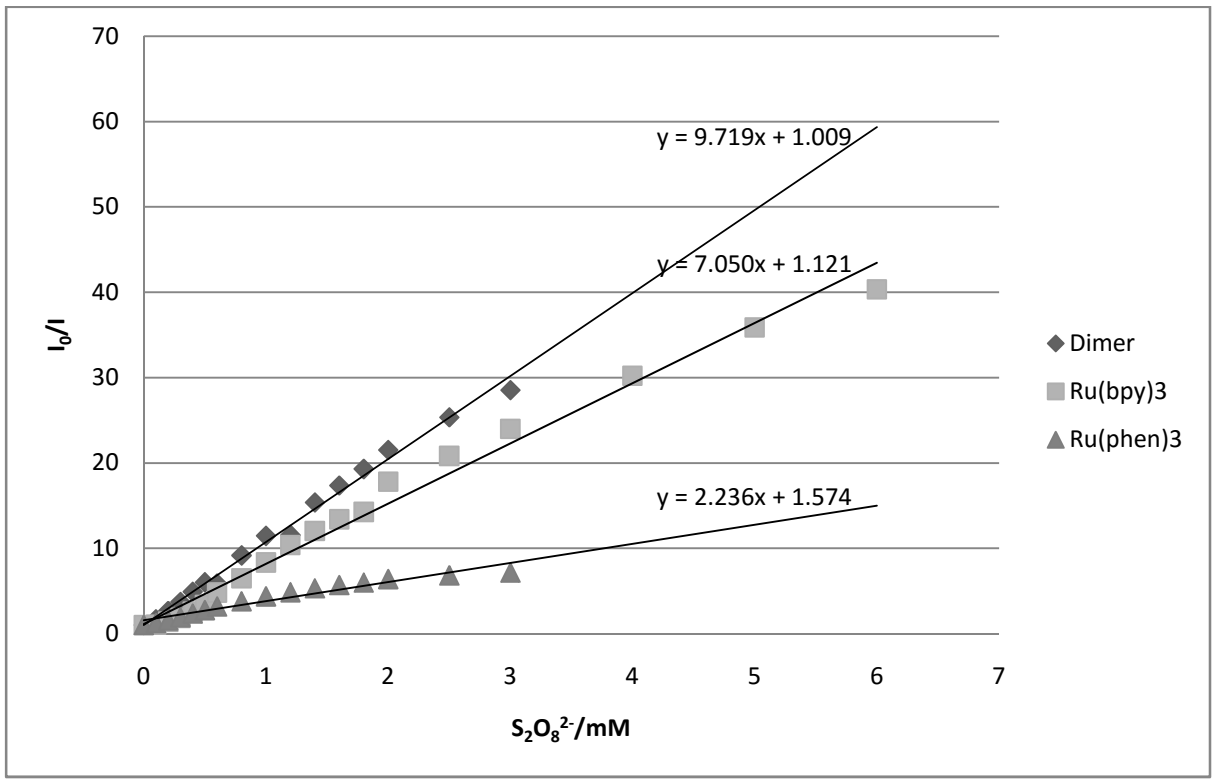
70
60
50
40
30
20
10
0
0
1
2
3
4
5
6
7
y = 9.719x + 1.009
y = 7.050x + 1.121
y = 2.236x + 1.574
I0/I
S2O8 2-/mM
Dimer
Ru(bpy)3
Ru(phen)3

Figure 3.17 Comparison of transient absorbance change at 450 nm of a solution of dimer and $Ru(phen)_3^{2+}$ in 0.2 M $(NH_4)_2SO_4$following a short laser pulse.

Figure 3.18 Comparison of transient absorbance change at 450 nm of a solution of dimer and $Ru(bpy)_3^{2+}$ in 0.2 M $(NH_4)_2SO_4$following a short laser pulse.

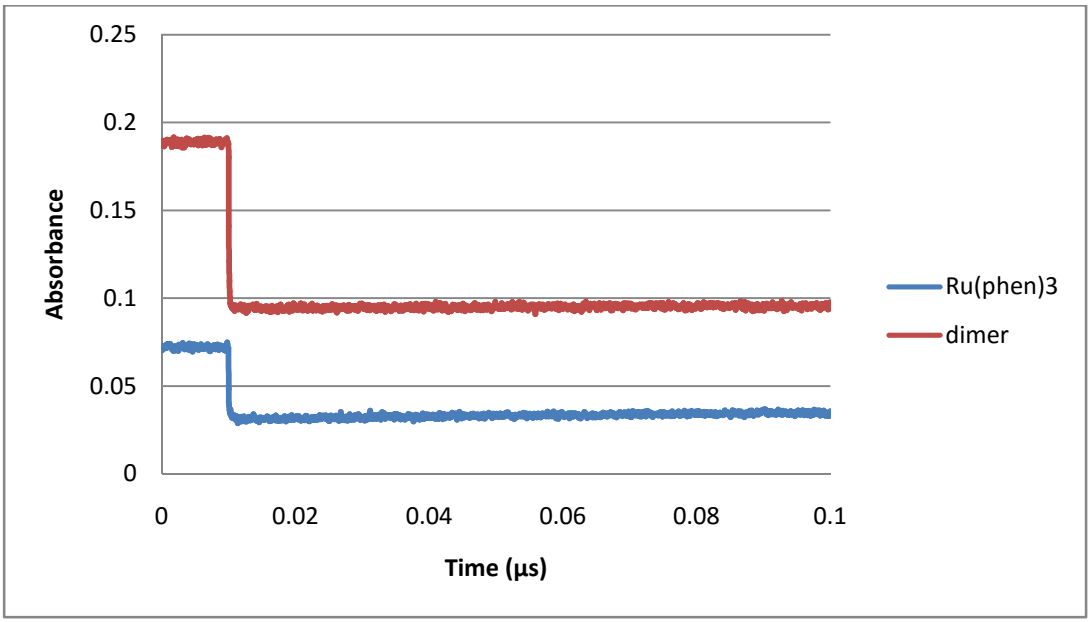
0.25
0.2
0.15
0.1
0.05
0
Absorbance
0
0.02
0.04
0.06
0.08
0.1
Time (µs)
Ru(phen)3
dimer

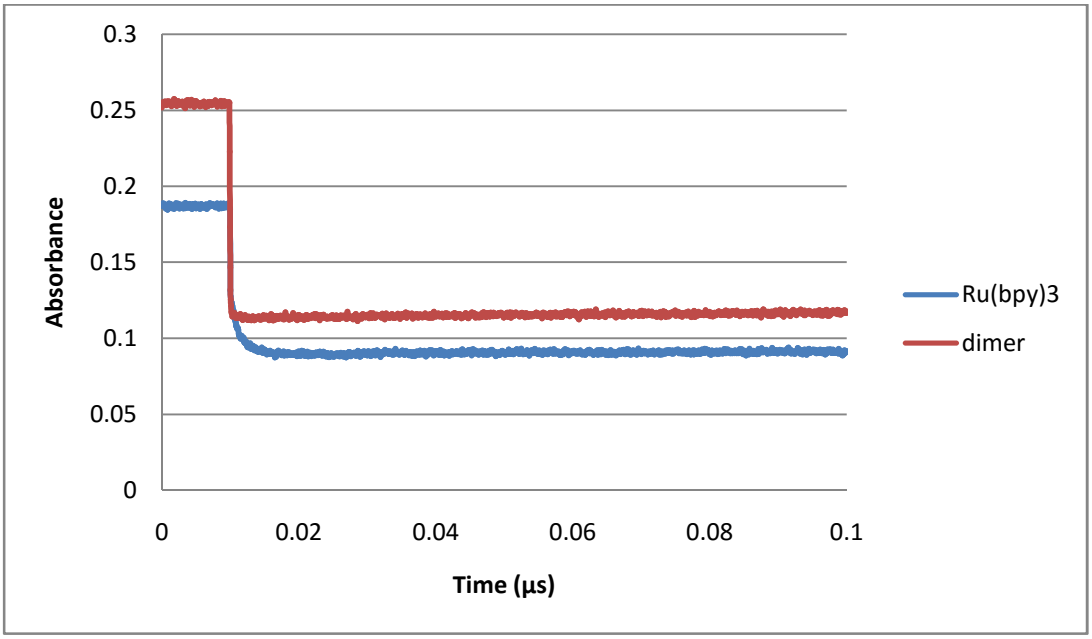
0.3
0.25
0.2
0.15
0.1
0.05
0
Absorbance
0
0.02
0.04
0.06
0.08
0.1
Time (µs)
Ru(bpy)3
dimer

Figure 3.19 Changes in absorbance following steady state irradiation of $Ru(phen)_3^{2+}$ in 0.2 M $(NH_4)_2SO_4$ containing 0.5 mM $S_2O_8^{2-}$.

Figure 3.20 Changes in Absorbance following steady state irradiation of the dimer in 0.2 M $(NH_4)_2SO_4$ containing 0.5 mM $S_2O_8^{2-}$.

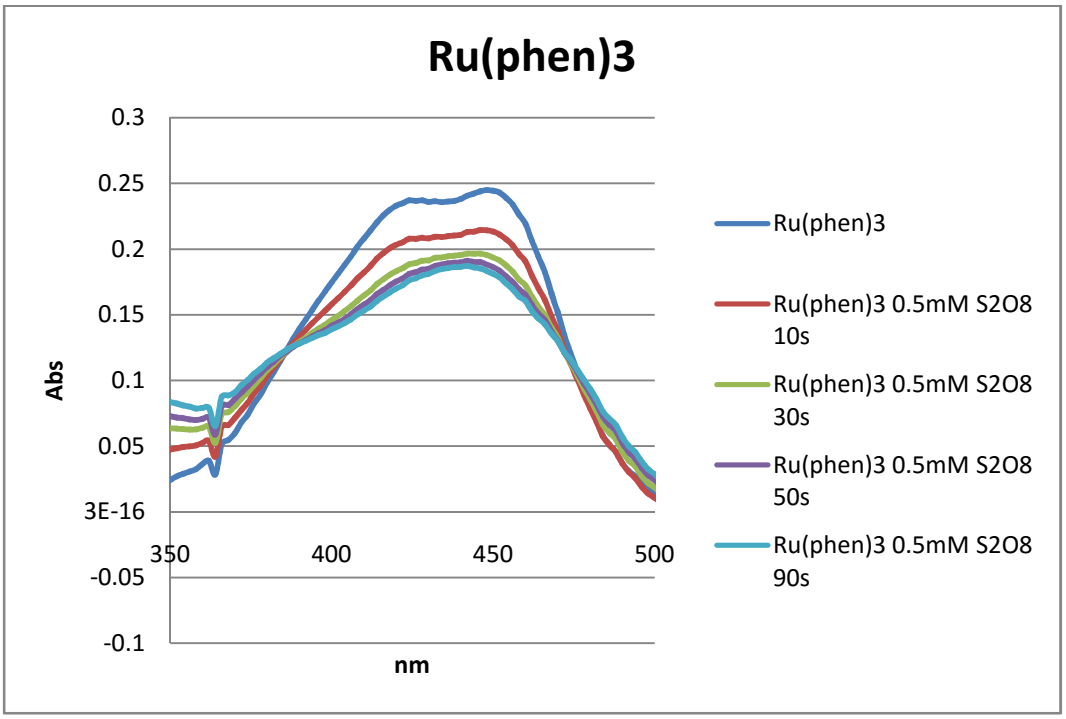
Ru(phen)3
0.3
0.25
0.2
0.15
0.1
0.05
3E-16
-0.05
-0.1
Abs
350
400
450
500
nm
Ru(phen)3
Ru(phen)3 0.5mM S2O8 10s
Ru(phen)3 0.5mM S2O8 30s
Ru(phen)3 0.5mM S2O8 50s
Ru(phen)3 0.5mM S2O8 90s

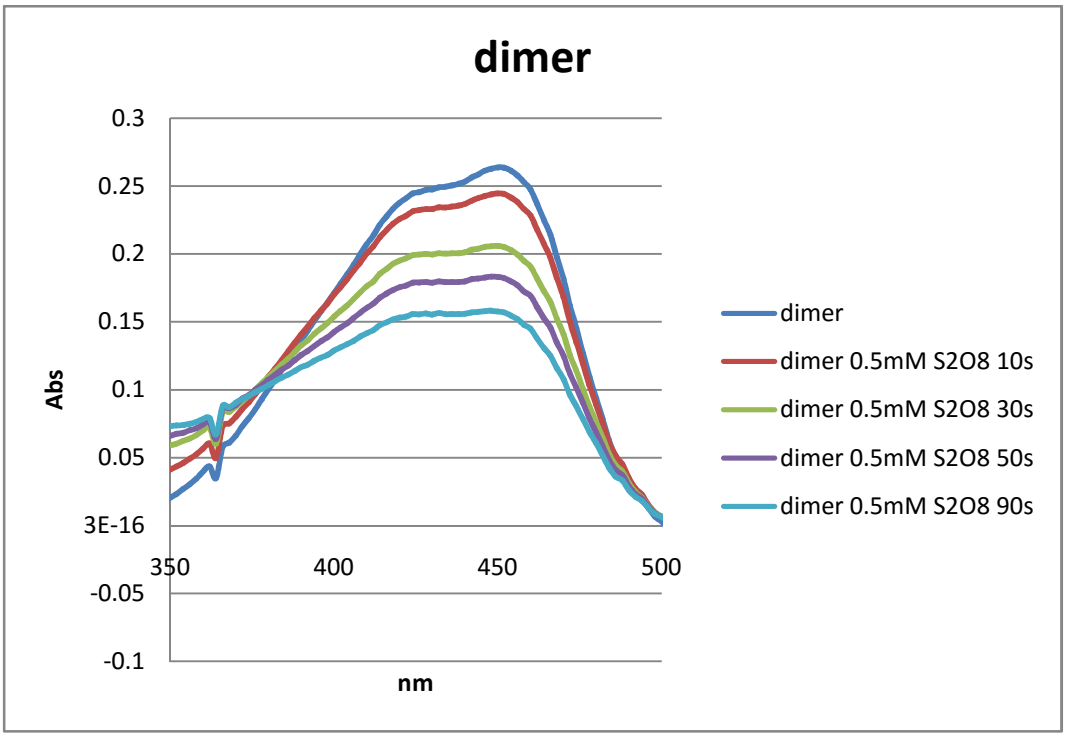
dimer
0.3
0.25
0.2
0.15
0.1
0.05
3E-16
-0.05
-0.1
Abs
350
400
450
500
nm
dimer
dimer 0.5mM S2O8 10s
dimer 0.5mM S2O8 30s
dimer 0.5mM S2O8 50s
dimer 0.5mM S2O8 90s

Figure 3.21 UV-vis spectrum of the dimer oxidized by Cl_2

Figure 3.22 UV-vis spectrum of the $Ru(bpy)_3^{2+}$ oxidized by Cl_2

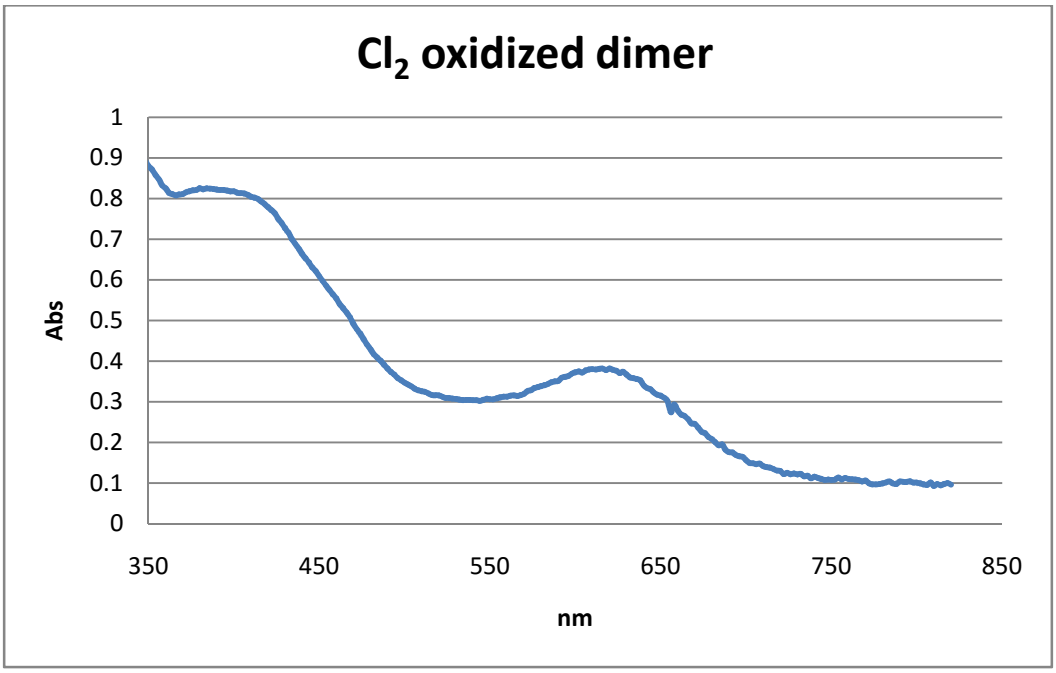
Cl2 oxidized dimer
Abs
1
0.9
0.8
0.7
0.6
0.5
0.4
0.3
0.2
0.1
0
350
450
550
650
750
850
nm

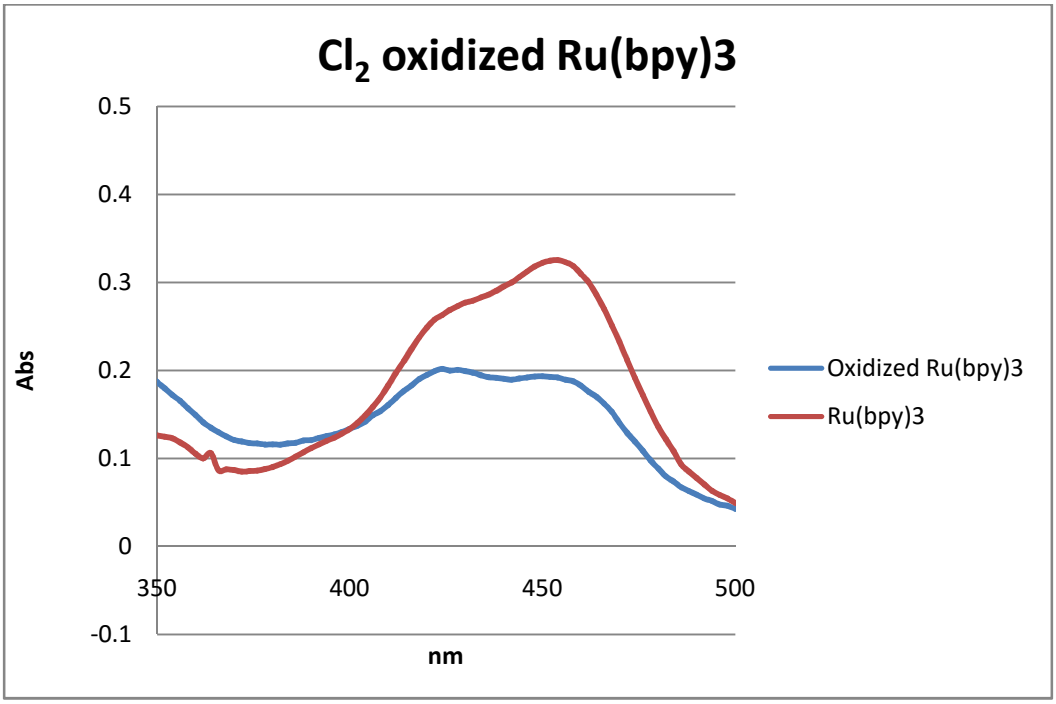
Cl2 oxidized Ru(bpy)3
Abs
0.5
0.4
0.3
0.2
0.1
0
-0.1
350
400
450
500
nm
Oxidized Ru(bpy)3
Ru(bpy)3

3.6 Reductive Quenching of Ru(II) Dimer and Monomers by Ascorbate

The quenching reactions of $Ru(bpy)_3^{2+}$, $Ru(phen)_3^{2+}$ and the dimer in aqueous solutions by ascorbate were investigated using traditional Stern-Volmer techniques and laser flash photolysis. The monomeric complexes have been previously investigated in detail and were used for comparison.

In the fluorescence measurements with ascorbate, the ruthenium complexes concentrations are enough to provide an absorbance of around 0.3, and the concentrations of ascorbate were varied from 0 to 0.1 mol L^{-1}. When excited with a wavelength of 450 nm, the ruthenium complexes have a strong fluorescence emission peaked at 605 nm. The addition of ascorbate caused a gradual decrease in the fluorescence intensity of ruthenium complexes and the emission had no shift.

Stern-Volmer plots for ascorbate quenching of ruthenium complexes fluorescence are shown in Figure 3.26. The result shows that the quenching constant (Figure 3.26 and Table 3.5), k_q, for the dimer is comparable to the k_q value for $Ru(phen)_3^{2+}$. This indicates that the monomeric complex and the dimeric complex behave similarly.

Table 3.5 Stern-Volmer quenching constants for the ruthenium complexes with ascorbate

pH	Ruthenium complexes	τ_0 (ns)	K_{sv} ($\times 10^3$ M^{-1})	k_q ($\times 10^8$ $M^{-1}s^{-1}$)
5	$[(phen)_2Ru(diphen)Ru(phen)_2]^{2+}$	1470	0.492	3.347
	$[Ru(phen)_3]^{2+}$	1000	0.324	3.324
	$[Ru(bpy)_3]^{2+}$	590	0.021	0.356

Figure 3.23 Effect of [ascorbate] on the emission intensity of the dimer in argon purged 0.2 M $(NH_4)_2SO_4$

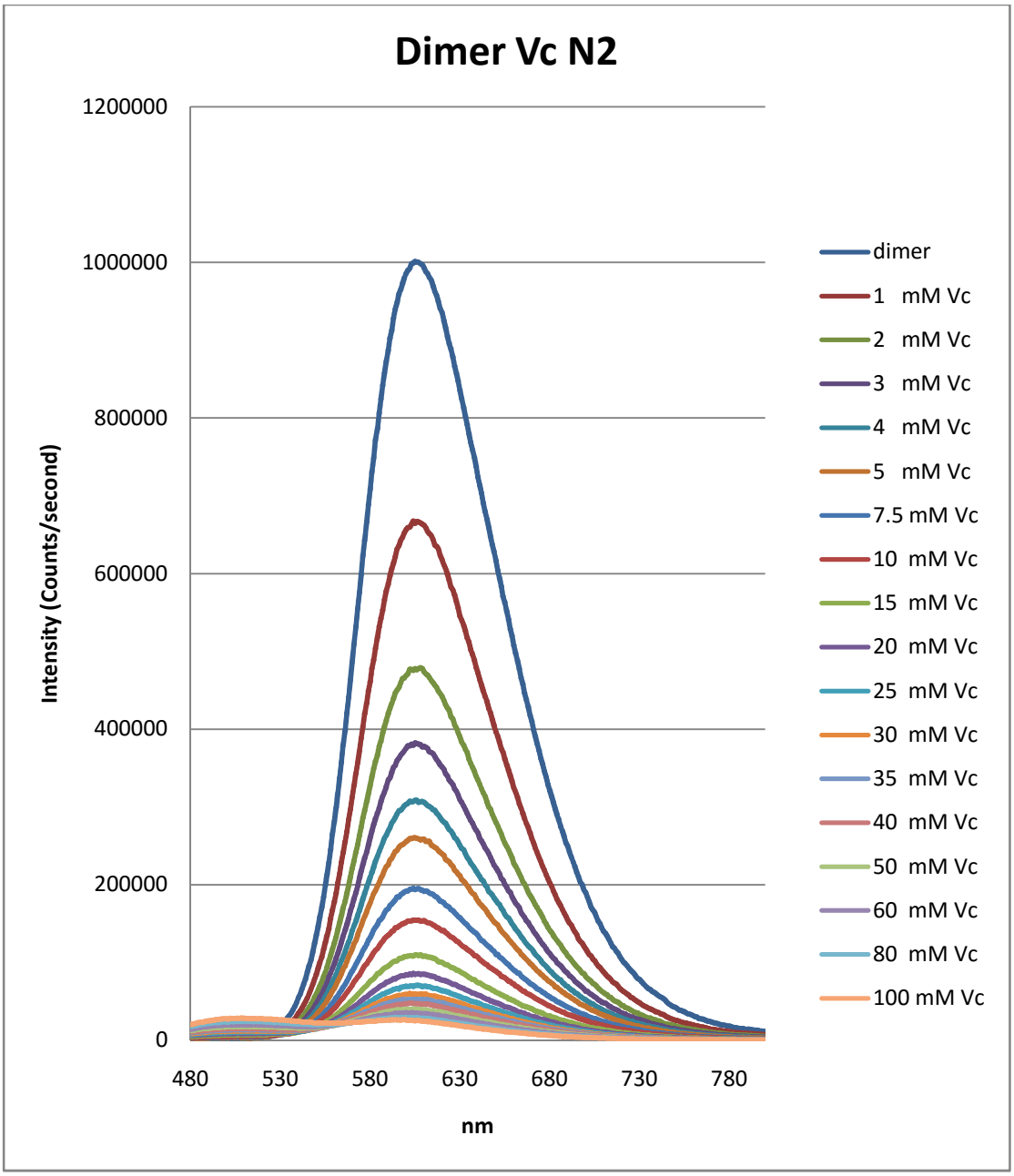
Dimer Vc N2
1200000
1000000
800000
600000
400000
200000
0
Intensity (Counts/second)
480
530
580
630
680
730
780
nm
dimer
1 mM Vc
2 mM Vc
3 mM Vc
4 mM Vc
5 mM Vc
7.5 mM Vc
10 mM Vc
15 mM Vc
20 mM Vc
25 mM Vc
30 mM Vc
35 mM Vc
40 mM Vc
50 mM Vc
60 mM Vc
80 mM Vc
100 mM Vc

Figure 3.24 Effect of ascorbate on the emission intensity of $Ru(phen)_3^{2+}$ in argon purged 0.2 M $(NH_4)_2SO_4$.

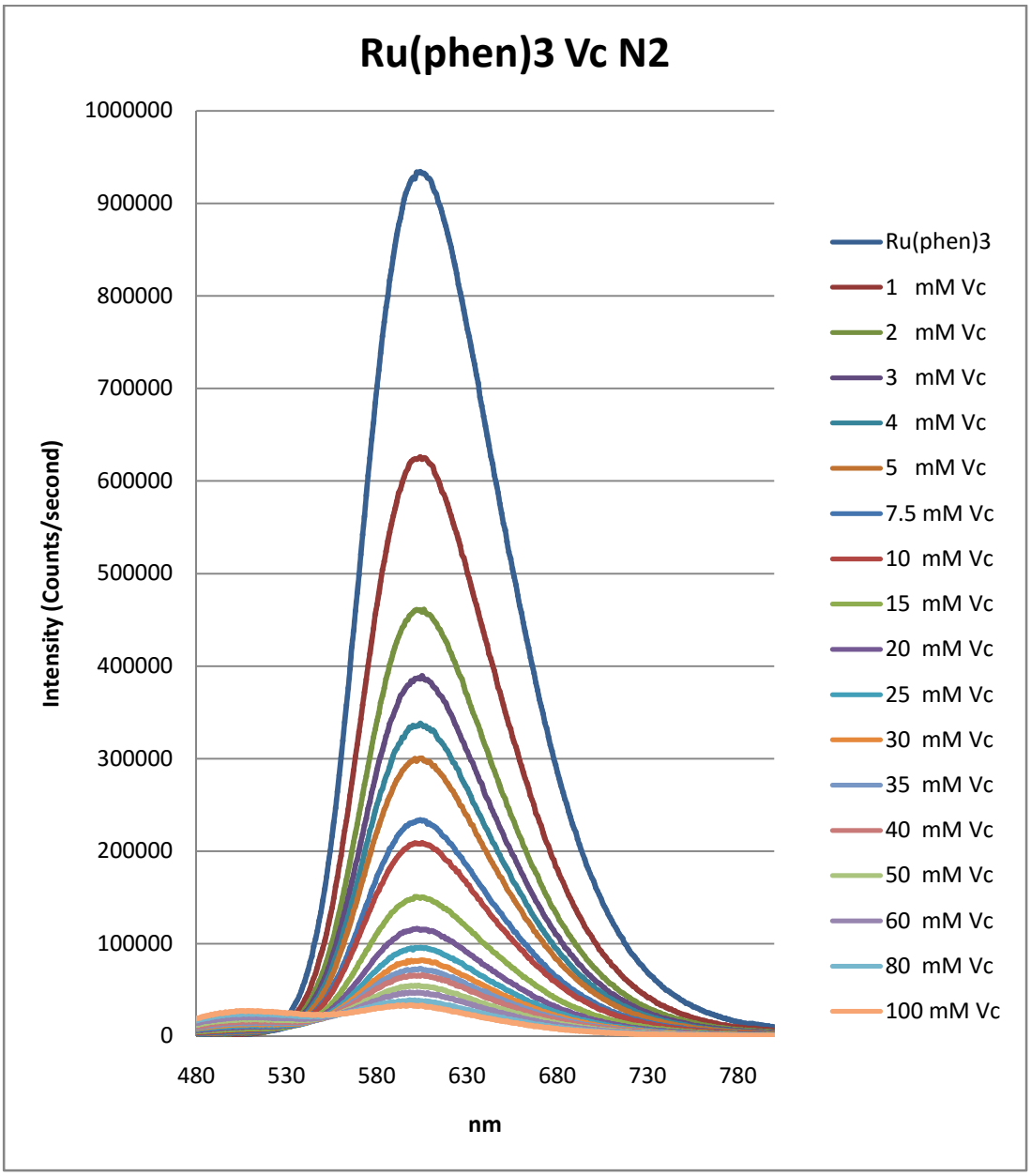
Ru(phen)3 Vc N2
Intensity (Counts/second)
1000000
900000
800000
700000
600000
500000
400000
300000
200000
100000
0
480
530
580
630
680
730
780
nm
Ru(phen)3
1 mM Vc
2 mM Vc
3 mM Vc
4 mM Vc
5 mM Vc
7.5 mM Vc
10 mM Vc
15 mM Vc
20 mM Vc
25 mM Vc
30 mM Vc
35 mM Vc
40 mM Vc
50 mM Vc
60 mM Vc
80 mM Vc
100 mM Vc

Figure 3.25 Effect of ascorbate on the emission intensity of $Ru(bpy)_3^{2+}$ in argon purged 0.2 M $(NH_4)_2SO_4$.

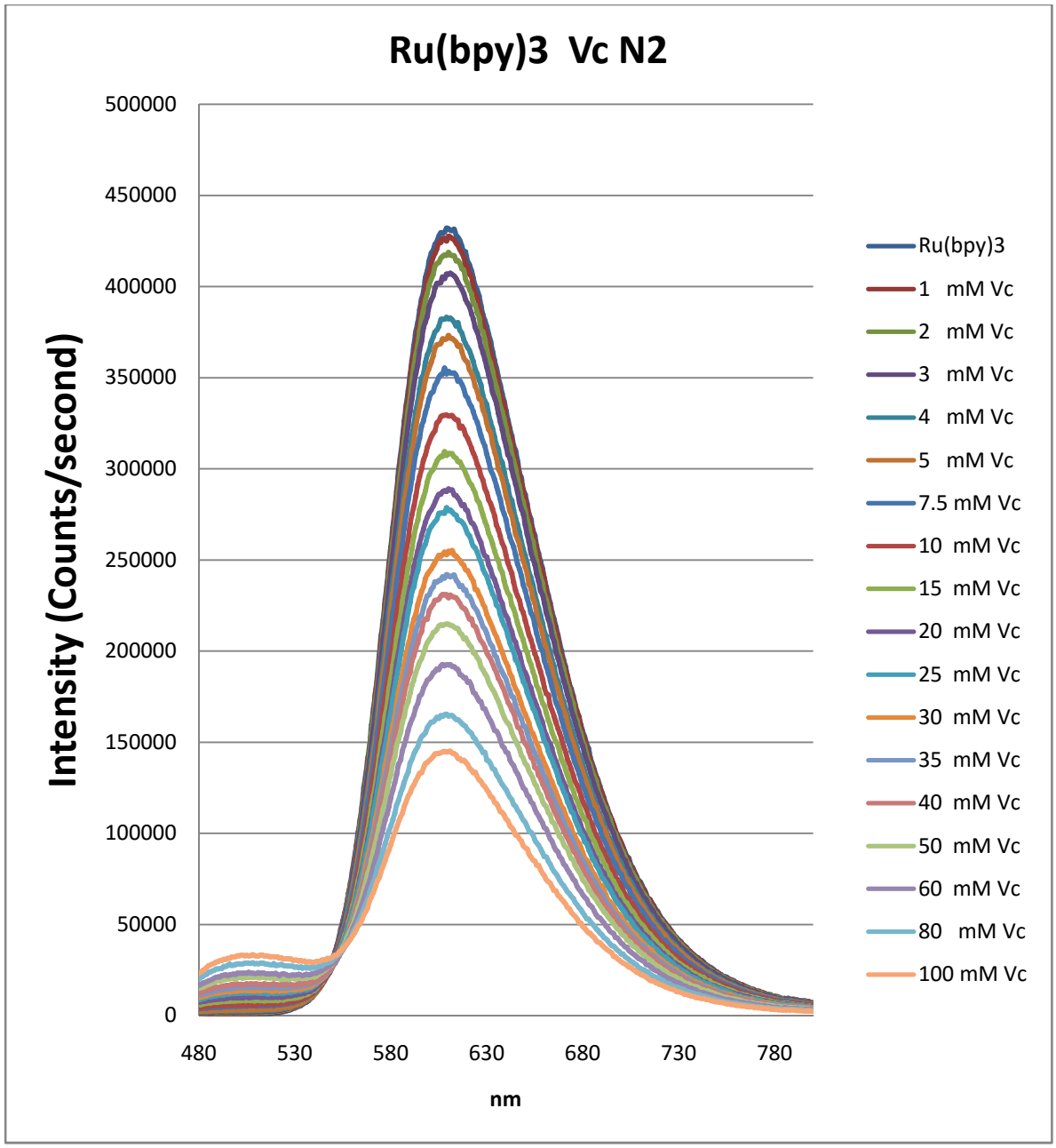
Ru(bpy)3 Vc N2
Intensity (Counts/second)
500000
450000
400000
350000
300000
250000
200000
150000
100000
50000
0
480
530
580
630
680
730
780
nm
Ru(bpy)3
1 mM Vc
2 mM Vc
3 mM Vc
4 mM Vc
5 mM Vc
7.5 mM Vc
10 mM Vc
15 mM Vc
20 mM Vc
25 mM Vc
30 mM Vc
35 mM Vc
40 mM Vc
50 mM Vc
60 mM Vc
80 mM Vc
100 mM Vc

Figure 3.26 Plots of the relative emission intensities of $Ru(bpy)_3^{2+}$, $Ru(phen)_3^{2+}$ and the dimer versus the ascorbate concentration. The solid lines and the associated equations were obtained using linear least squares and are the "best" fits.

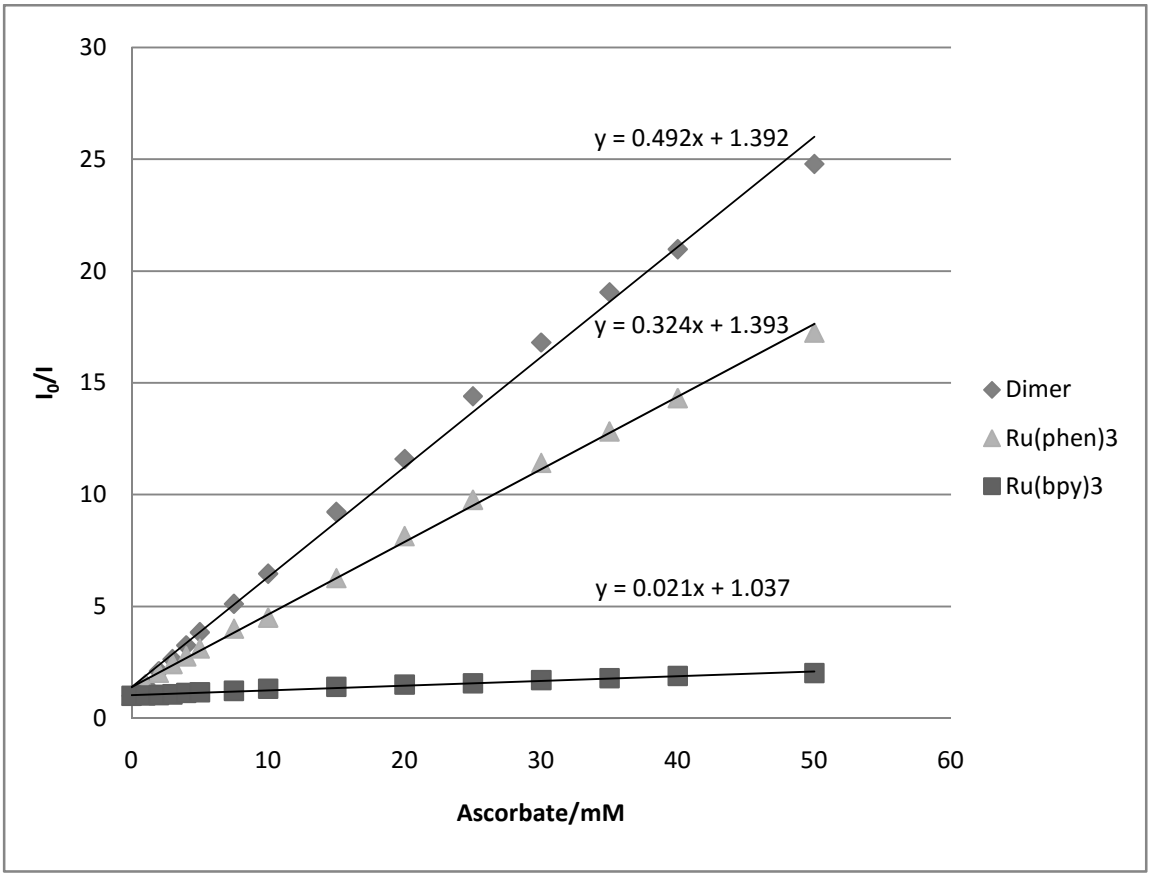
30
25
20
15
10
5
0
0
10
20
30
40
50
60
I_0/I
Ascorbate/mM
y = 0.492x + 1.392
y = 0.324x + 1.393
y = 0.021x + 1.037
Dimer
Ru(phen)3
Ru(bpy)3

Figure 3.27 Representative absorption transient for ruthenium complexes with ascorbate

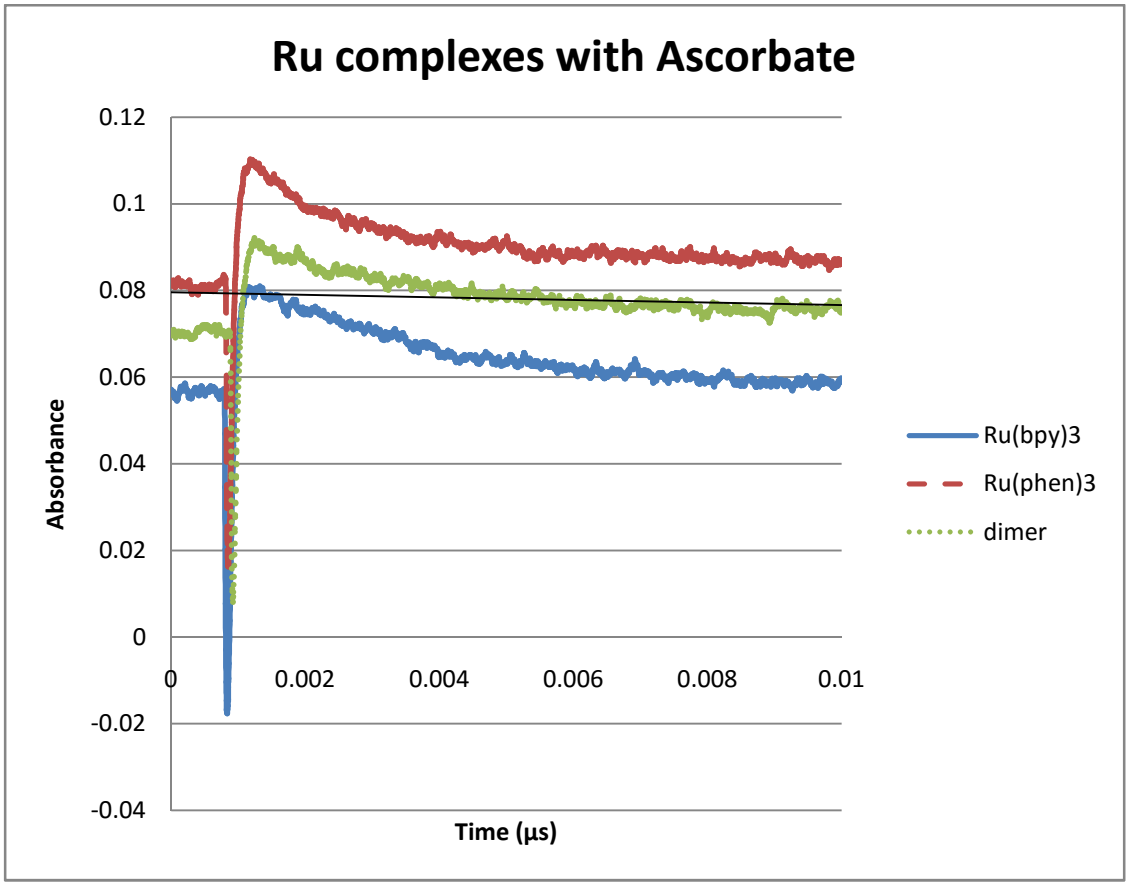
Ru complexes with Ascorbate
0.12
0.1
0.08
0.06
0.04
0.02
0
-0.02
-0.04
Absorbance
0
0.002
0.004
0.006
0.008
0.01
Time (µs)
Ru(bpy)3
Ru(phen)3
dimer

Chapter 4 Conclusions

4.1 Synthesis of the Bridging Ligand

The bridging ligand was prepared using a method recently optimized by Puckett. Additional optimization pointed out the critical nature of the oxygen sensitivity of the reaction and led to a reliable procedure with an average yield of approximately 40%. In addition work-up conditions were found that provided a product that was completely free from triphenylphosphine which had been a problem in past work. With a good source of product available several attempts were made to obtain crystals suitable for single crystal diffraction. Fortunately, the efforts proved successful and good quality crystals were sent for analysis.

4.2 Crystal structureof 5,5'-Bi-1,10-phenanthroline (diphen)

Bond lengths and bond angles for phen were chosen from a shallow-boat shape, all the six-membered rings are exactly planar. Therefore, phen exhibits good symmetry with the identical in above and bottom half.

In the two columns of Table 4.1 the bond lengths and bond angles are compared with the phen literature values by Satoshi Nishigaki.[44] The agreement is fairly good, except for the bonds contain C12, whose lengths are somewhat larger than the phen. The bond length for C12-C12, which linked two phen subunits, is 1.494(3) Å, longer than the average bond lengths for N-C (1.326 Å) or C-C (1.372 Å)[45] in the literature for phen-coordinated metal complexes. This reflects that the bridging bond between two phen subunits is stretched and also caused the neighbor rings slightly stretched.

Table 4.1 Selected bond lengths (Å) and band angles (°) for diphen and phen

Bond lengths (Å)	diphen	phen
N1-C1	1.325(2)	1.317(7)
C1-C2	1.403(3)	1.402(11)
C3-C2	1.369(3)	1.352(11)
C4-C3	1.412(2)	1.410(9)
C4-C11	1.435(2)	1.427(10)
C12-C11	1.357(2)	1.330(12)
C12-C7	1.451(2)	1.426(12)
C7-C8	1.412(3)	1.414(11)
C8-C9	1.371(3)	1.348(13)
C9-C10	1.405(3)	1.394(12)
N2-C10	1.321(2)	1.312(8)
Band angles (°)		
N1-C1-C2	123.78(17)	123.8(6)
C3-C2-C1	119.39(17)	118.9(6)
C2-C3-C4	118.68(17)	119.0(7)
C3-C4-C11	122.04(16)	124.2(7)
C12-C11-C4	121.51(16)	122.5(8)
C11-C12-C7	119.79(16)	120.9(6)
C8-C7-C12	122.77(17)	124.5(6)
C9-C8-C7	120.02(18)	122.2(7)
C8-C9-C10	118.23(17)	116.9(7)
N2-C10-C9	123.86(17)	125.1(8)

Figure 4.1 Left: The model of the diphen single-crystal structure. Anions are omitted for clarity. Atom color code: carbon, grey; nitrogen, blue. Right: The structure for phen

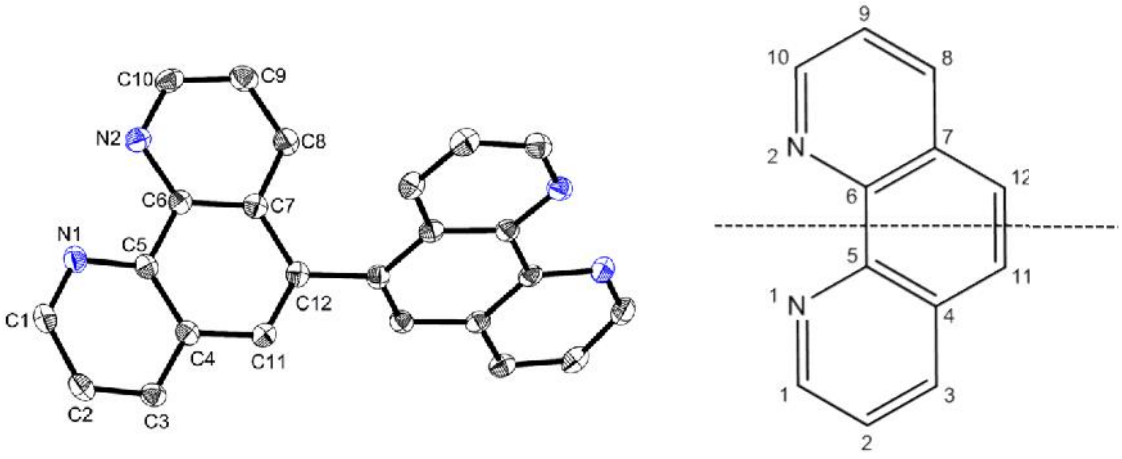

4.3 Synthesis of $[(phen)_2Ru\text{-}diphen\text{-}Ru(phen)_2](PF_6)_4$ complexes.

Synthesis of this dimer utilized a commonly used polymeric ruthenium carbonyl compound as the entry point. This entry point was chosen because the polymeric material readily reacts with one chelating ligand such are 1,10-phenanthroline under very mild conditions with no further reaction. Reaction with diphen yields a bridged dimer. Further reaction with additional ligands requires the remaining carbonyl groups be removed with trimethylamine-N-oxide. The product was fully characterized as described earlier. As expected the dimer shares many common features with $Ru(phen)_3^{2+}$.For example the maximum absorbance in the visible region of the spectrum occurs are 446 nm with the dimer and at 448 with the monomer. Emission maxima are identical at room temperature.

4.4 Quenching of $[(phen)_2Ru(diphen)Ru(phen)_2]Cl_4$ by Peroxydisulfate

The photoredox reactions of $[(phen)_2Ru(diphen)Ru(phen)_2]Cl_4$ were studied through a series of quenching reactions. The analogous monomeric complexes $Ru(bpy)_3^{2+}$ and $Ru(phen)_3^{2+}$

were used as comparisons. In previous research, Fe^{3+} was used as an oxidative quencher in 0.5 M H_2SO_4. Laser flash photolysis measurements under conditions where more than 50 % of $Ru(bpy)_3^{2+}$ was quenched to yield $Ru(bpy)_3^{3+}$ consistently indicated the yield of oxidized $[(phen)_2Ru(diphen)Ru(phen)_2]^{4+}$ was limited to less than 50 %. It appears at this time that oxidation of one half of the dimer prevents the quenching reaction by the other half.

Quenching of $Ru(bpy)_3^{2+}$ or $Ru(phen)_3^{2+}$ by peroxydisulfate ion is known to proceed with a quantum yield of 2. The standard reduction potential for the two electron reduction of peroxydisulfate anion to the sulfate anion:

$E^0(S_2O_8^{2-}/2SO_4^{2-}) = 1.94$ V

The standard reduction potential for the reduction of $S_2O_8^{2-}$ to $SO_4^{-}\cdot$ occurs at a lower potential:

$E^0(S_2O_8^{2-}/SO_4^{-}\cdot, SO_4^{2-}) = 1.45$ V

The sulfate radical anion generated from one-electron reduction of $S_2O_8^{2-}$ is a stronger oxidant with an oxidation potential of 2.44 V:

$E^0(SO_4^{-}\cdot/SO_4^{2-}) = 2.44$ V

The reaction of excited state of $Ru(bpy)_3^{2+}$ with $S_2O_8^{2-}$ to produce Ru(III) species has been investigated by Bolletta.[46] The following photoinduced oxidation scheme appears to describe the high yield

$$Ru(bpy)_3^{2+} \xrightarrow{h\nu} Ru(bpy)_3^{2+*} \qquad \text{eq. 4.2.2}$$

$$Ru(bpy)_3^{2+*} + S_2O_8^{2-} \xrightarrow{kq} Ru(bpy)_3^{3+} + SO_4^{-}\cdot + SO_4^{2-} \qquad \text{eq. 4.2.3}$$

$$Ru(bpy)_3^{2+} + SO_4^{-}\cdot \xrightarrow{fast} Ru(bpy)_3^{3+} + SO_4^{2-} \qquad \text{eq. 4.2.4}$$

A strong oxidizing intermediate, $SO_4^{-}\cdot$, is produced during the reaction (eq 4.2.3) which generates a second Ru(III) (eq 4) through a thermal reaction. Previous reports show that the initial photoinduced electron transfer occurs in a collision between excited $Ru(bpy)_3^{2+*}$ and $S_2O_8^{2-}$ in the $Ru(bpy)_3^{2+}$– $S_2O_8^{2-}$ system[46-47].

Unlike the mononuclear ruthenium (II) complex, $Ru(bpy)_3^{2+}$, the symmetric dimer contains two reducing sites. These two sites are potentially capable of reducing $S_2O_8^{2-}$ through a single two-electron reaction, or sequence of two one-electron reactions. The reactions of interest in this system are shown below.

$$Ru(II)\text{-}Ru(II) + S_2O_8^{2-} \longrightarrow Ru(III)\text{-}Ru(III) + 2SO_4^{2-} \qquad \text{eq. 4.2.5}$$

A Stern-Volmer investigation of the quenching reaction indicted that the dimer had a higher Stern-Volmer quenching constant, k_q, than $Ru(phen)_3^{2+}$. One possible explanation is simply the difference in charge of the complexes. Since the quencher has a negative charge it is reasonable to assume that electrostatics will play a significant role in the quenching reaction.

The most interesting result that may have a bearing on the mechanism is the laser flash photolysis transients. Figure 3.18 shows a clear step function with the dimer. On the other hand the transient absorbance changes with $Ru(bpy)_3^{2+}$ clearly show a biphasic reaction. The first is very fast and is probably the initial quenching reaction. The second slower phase can be interpreted as the diffusion of the sulfate radical ion to another reduced complex. Since the dimer has a second ruthenium in close proximity it is reasonable to assume that the diffusion to the adjacent ruthenium center will be very fast and appear as a single step function. Unfortunately, these observations were made during the data analysis and it was not possible to

examine the reactions on a shorter time scale. Figure 3.17, however does give a small indication that a similar slow phase is present in $Ru(phen)_3^{2+}$.

4.5 Quenching of $[(phen)_2Ru(diphen)Ru(phen)_2]Cl_4$ by Ascorbate

A Stern-Volmer investigation of the quenching reaction indicted that the dimer had a similar Stern-Volmer quenching constant k_q with $Ru(phen)_3^{2+}$. In the laser flash photolysis transients, there is no big difference between the absorbance changes of the dimer and $Ru(phen)_3^{2+}$. The possible explanation is ascorbate is different from $S_2O_8^{2-}$, one ascorbate molecular only can donate one electron to ruthenium complexes. Here so after the half of the dimer was reduced, the other half had no advantage to be reduced when compare with monomers.

References

1. (a) Williams, R., BECQUEREL PHOTOVOLTAIC EFFECT IN BINARY COMPOUNDS. *Journal of Chemical Physics* **1960,** *32* (5), 1505-1514; (b) Becquerel, E., Memoire sur les effets electriques produis sous I'influence des reyons solaires. *Comptes Rendus* **1839,** *9*, 561-567.

2. Oregan, B.; Gratzel, M., A LOW-COST, HIGH-EFFICIENCY SOLAR-CELL BASED ON DYE-SENSITIZED COLLOIDAL TIO2 FILMS. *Nature* **1991,** *353* (6346), 737-740.

3. (a) Amadelli, R.; Argazzi, R.; Bignozzi, C. A.; Scandola, F., DESIGN OF ANTENNA-SENSITIZER POLYNUCLEAR COMPLEXES - SENSITIZATION OF TITANIUM-DIOXIDE WITH RU(BPY)2(CN)2 2RU(BPY(COO)2)22. *Journal of the American Chemical Society* **1990,** *112* (20), 7099-7103; (b) Nazeeruddin, M. K.; Liska, P.; Moser, J.; Vlachopoulos, N.; Gratzel, M., CONVERSION OF LIGHT INTO ELECTRICITY WITH TRINUCLEAR RUTHENIUM COMPLEXES ADSORBED ON TEXTURED TIO2 FILMS. *Helvetica Chimica Acta* **1990,** *73* (6), 1788-1803.

4. Nicewicz, D. A.; MacMillan, D. W. C., Merging photoredox catalysis with organocatalysis: The direct asymmetric alkylation of aldehydes. *Science* **2008,** *322* (5898), 77-80.

5. (a) Cady, C. W.; Crabtree, R. H.; Brudvig, G. W., Functional models for the oxygen-evolving complex of photosystem II. *Coordination Chemistry Reviews* **2008,** *252* (3-4), 444-455; (b) Yamazaki, H.; Shouji, A.; Kajita, M.; Yagi, M., Electrocatalytic and photocatalytic water oxidation to dioxygen based on metal complexes. *Coordination Chemistry Reviews* **2010,** *254* (21-22), 2483-2491.

6. (a) Yagi, M.; Tajima, S.; Komi, M.; Yamazaki, H., Highly active and tunable catalysts for O-2 evolution from water based on mononuclear ruthenium(II) monoaquo complexes. *Dalton Transactions* **2011,** *40* (15), 3802-3804; (b) Duan, L.; Araujo, C. M.; Ahlquist, M. S. G.; Sun, L., Highly efficient and robust molecular ruthenium catalysts for water oxidation. *Proceedings of the National Academy of Sciences of the United States of America* **2012,** *109* (39), 15584-15588; (c) Duan, L.; Bozoglian, F.; Mandal, S.; Stewart, B.; Privalov, T.; Llobet, A.; Sun, L., A molecular ruthenium catalyst with water-oxidation activity comparable to that of photosystem II. *Nature Chemistry* **2012,** *4* (5), 418-423.

7. Sens, C.; Romero, I.; Rodriguez, M.; Llobet, A.; Parella, T.; Benet-Buchholz, J., A new Ru complex capable of catalytically oxidizing water to molecular dioxygen. *Journal of the American Chemical Society* **2004,** *126* (25), 7798-7799.

8. Esposito, D. V.; Hunt, S. T.; Stottlemyer, A. L.; Dobson, K. D.; McCandless, B. E.; Birkmire, R. W.; Chen, J. G. G., Low-Cost Hydrogen-Evolution Catalysts Based on Monolayer Platinum on Tungsten Monocarbide Substrates. *Angewandte Chemie-International Edition* **2010,** *49* (51), 9859-9862.

9. (a) Balzani, V.; Juris, A., Photochemistry and photophysics of Ru(II)-polypyridine complexes in the Bologna group. From early studies to recent developments. *Coordination*

Chemistry Reviews **2001,** *211*, 97-115; (b) Howerton, B. S.; Heidary, D. K.; Glazer, E. C., Strained Ruthenium Complexes Are Potent Light-Activated Anticancer Agents. *Journal of the American Chemical Society* **2012,** *134* (20), 8324-8327; (c) Hirahara, M.; Ertem, M. Z.; Komi, M.; Yamazaki, H.; Cramer, C. J.; Yagi, M., Mechanisms of Photoisomerization and Water-Oxidation Catalysis of Mononuclear Ruthenium(II) Monoaquo Complexes. *Inorganic Chemistry* **2013,** *52* (11), 6354-6364.

10. (a) Crosby, G. A.; Perkins, W. G.; Klassen, D. M., LUMINESCENCE FROM TRANSITION-METAL COMPLEXES - TRIS(2,2'-BIPYRIDINE)- AND TRIS(1,10-PHENANTHROLINE)RUTHENIUM(2). *Journal of Chemical Physics* **1965,** *43* (5), 1498-+; (b) Crosby, G. A.; Watts, R. J.; Carstens, D. H., INVERSION OF EXCITED STATES OF TRANSITION-METAL COMPLEXES. *Science* **1970,** *170* (3963), 1195-&.

11. (a) Ciamician, G., THE PHOTOCHEMISTRY OF THE FUTURE. *Science (New York, N.Y.)* **1912,** *36* (926), 385-94; (b) Roth, H. D., THE BEGINNINGS OF ORGANIC-PHOTOCHEMISTRY. *Angewandte Chemie-International Edition in English* **1989,** *28* (9), 1193-1207.

12. Krause, R. A.; Krause, K., CHEMISTRY OF BIPYRIDYL-LIKE LIGANDS - ISOMERIC COMPLEXES OF RUTHENIUM(II) WITH 2-(PHENYLAZO)PYRIDINE. *Inorganic Chemistry* **1980,** *19* (9), 2600-2603.

13. Lytle, F. E.; Hercules, D. M., LUMINESCENCE OF TRIS(2,2'-BIPYRIDINE)RUTHENIUM(2) DICHLORIDE. *Journal of the American Chemical Society* **1969,** *91* (2), 253-&.

14. Kalyanasundaram, K., PHOTOPHYSICS, PHOTOCHEMISTRY AND SOLAR-ENERGY CONVERSION WITH TRIS(BIPYRIDYL)RUTHENIUM(II) AND ITS ANALOGS. *Coordination Chemistry Reviews* **1982,** *46* (OCT), 159-244.

15. McCusker, J. K., Femtosecond absorption spectroscopy of transition metal charge-transfer complexes. *Accounts of Chemical Research* **2003,** *36* (12), 876-887.

16. Juris, A.; Balzani, V.; Barigelletti, F.; Campagna, S.; Belser, P.; Vonzelewsky, A., RU(II) POLYPYRIDINE COMPLEXES - PHOTOPHYSICS, PHOTOCHEMISTRY, ELECTROCHEMISTRY, AND CHEMI-LUMINESCENCE. *Coordination Chemistry Reviews* **1988,** *84*, 85-277.

17. Teply, F., PHOTOREDOX CATALYSIS BY Ru(bpy)(3) (2+) TO TRIGGER TRANSFORMATIONS OF ORGANIC MOLECULES. ORGANIC SYNTHESIS USING VISIBLE-LIGHT PHOTOCATALYSIS AND ITS 20th CENTURY ROOTS. *Collection of Czechoslovak Chemical Communications* **2011,** *76* (7), 859-917.

18. Durham, B.; Millett, F., Ruthenium(II) polypyridine complexes and the electron-transfer reactions of metalloproteins. *Journal of Chemical Education* **1997,** *74* (6), 636-640.

19. Yonemoto, E. H.; Riley, R. L.; Kim, Y. I.; Atherton, S. J.; Schmehl, R. H.; Mallouk, T. E., PHOTOINDUCED ELECTRON-TRANSFER IN COVALENTLY LINKED RUTHENIUM TRIS(BIPYRIDYL) VIOLOGEN MOLECULES - OBSERVATION OF BACK ELECTRON-TRANSFER IN THE MARCUS INVERTED REGION. *Journal of the American Chemical Society* **1992,** *114* (21), 8081-8087.

20. Young, R. C.; Meyer, T. J.; Whitten, D. G., KINETIC RELAXATION MEASUREMENT OF RAPID ELECTRON-TRANSFER REACTIONS BY FLASH-PHOTOLYSIS - CONVERSION OF LIGHT ENERGY INTO CHEMICAL ENERGY USING RU(BPY)33+-RU(BPY)32+STAR COUPLE. *Journal of the American Chemical Society* **1975,** *97* (16), 4781-4782.

21. Durham, B.; Millett, F., Design of photoactive ruthenium complexes to study electron transfer and proton pumping in cytochrome oxidase. *Biochimica Et Biophysica Acta-Bioenergetics* **2012,** *1817* (4), 567-574.

22. Hatefi, Y., The Mitochondrial Electron Transport and Oxidative Phosohorylation System. *Ann. Rev. Biochem* **1985,** *54*, 1015-69.

23. Hatefi, Y.; Griffiths, D. E.; Haavik, A. G., RECONSTITUTION OF ELECTRON TRANSPORT SYSTEM .1. PREPARATION AND PROPERTIES OF INTERACTING ENZYME COMPLEXES. *Biochemical and Biophysical Research Communications* **1961,** *4* (6), 441-&.

24. Leung, K. H.; Hinkle, P. C., RECONSTITUTION OF ION-TRANSPORT AND RESPIRATORY CONTROL IN VESICLES FORMED FROM REDUCED COENZYME Q CYTOCHROME-C REDUCTASE AND PHOSPHOLIPIDS. *Journal of Biological Chemistry* **1975,** *250* (21), 8467-8471.

25. Moore, G. R.; Pettigrew, G. W., Cytochromes c. Evolutionary, structural and physicochemical aspects. *Cytochromes c. Evolutionary, structural and physicochemical aspects.* **1990**, i-xvi, 1-478.

26. (a) Pan, L. P.; Durham, B.; Wolinska, J.; Millett, F., PREPARATION AND CHARACTERIZATION OF SINGLY LABELED RUTHENIUM POLYPYRIDINE CYTOCHROME-C DERIVATIVES. *Biochemistry* **1988,** *27* (19), 7180-7184; (b) Olabe, J. A.; Haim, A., AN EXAMPLE OF INTRAMOLECULAR ELECTRON-TRANSFER ASSISTANCE IN A BIMOLECULAR REDOX REACTION - PEROXYDISULFATE OXIDATION OF (MU-1,2-BIS(4-PYRIDYL)ETHANE)PENTAAMMINERUTHENIUM(III) PENTACYANOFERRATE(II) VIA ITS ELECTRONIC ISOMER. *Inorganic Chemistry* **1989,** *28* (17), 3277-3278; (c) Liu, R. Q.; Geren, L.; Anderson, P.; Fairris, J. L.; Peffer, N.; McKee, A.; Durham, B.; Millett, F., DESIGN OF RUTHENIUM-CYTOCHROME-C DERIVATIVES TO MEASURE ELECTRON-TRANSFER TO CYTOCHROME-C PEROXIDASE. *Biochimie* **1995,** *77* (7-8), 549-561; (d) Zaslavsky, D.; Sadoski, R. C.; Rajagukguk, S.; Geren, L.; Millett, F.; Durham, B.; Gennis, R. B., Direct measurement of proton release by cytochrome c oxidase in

solution during the F -> O transition. *Proceedings of the National Academy of Sciences of the United States of America* **2004,** *101* (29), 10544-10547.

27. Pan, L. P.; Hibdon, S.; Liu, R. Q.; Durham, B.; Millett, F., INTRACOMPLEX ELECTRON-TRANSFER BETWEEN RUTHENIUM-CYTOCHROME-C DERIVATIVES AND CYTOCHROME-C-OXIDASE. *Biochemistry* **1993,** *32* (33), 8492-8498.

28. Brand, S. E.; Rajagukguk, S.; Ganesan, K.; Geren, L.; Fabian, M.; Han, D.; Gennis, R. B.; Durham, B.; Millett, F., A new ruthenium complex to study single-electron reduction of the pulsed OH state of detergent-solubilized cytochrome oxidase. *Biochemistry* **2007,** *46* (50), 14610-14618.

29. Tommos, C.; Babcock, G. T., Oxygen production in nature: A light-driven metalloradical enzyme process. *Accounts of Chemical Research* **1998,** *31* (1), 18-25.

30. (a) Brunschwig, B. S.; Chou, M. H.; Creutz, C.; Ghosh, P.; Sutin, N., MECHANISMS OF WATER OXIDATION TO OXYGEN - COBALT(IV) AS AN INTERMEDIATE IN THE AQUOCOBALT(II)-CATALYZED REACTION. *Journal of the American Chemical Society* **1983,** *105* (14), 4832-4833; (b) Harriman, A.; Porter, G.; Walters, P., PHOTOOXIDATION OF WATER TO OXYGEN SENSITIZED BY TRIS(2,2'-BIPYRIDYL)RUTHENIUM(II). *Journal of the Chemical Society-Faraday Transactions Ii* **1981,** *77*, 2373-2383.

31. (a) Harriman, A.; Richoux, M. C.; Christensen, P. A.; Mosseri, S.; Neta, P., REDOX REACTIONS WITH COLLOIDAL METAL-OXIDES - COMPARISON OF RADIATION-GENERATED AND CHEMICALLY GENERATED RUO2.2H2O AND MNO2 COLLOIDS. *Journal of the Chemical Society-Faraday Transactions I* **1987,** *83*, 3001-3014; (b) Hara, M.; Waraksa, C. C.; Lean, J. T.; Lewis, B. A.; Mallouk, T. E., Photocatalytic water oxidation in a buffered tris(2,2 '-bipyridyl)ruthenium complex-colloidal IrO2 system. *Journal of Physical Chemistry A* **2000,** *104* (22), 5275-5280.

32. (a) Sala, X.; Romero, I.; Rodriguez, M.; Escriche, L.; Llobet, A., Molecular Catalysts that Oxidize Water to Dioxygen. *Angewandte Chemie-International Edition* **2009,** *48* (16), 2842-2852; (b) Concepcion, J. J.; Jurss, J. W.; Brennaman, M. K.; Hoertz, P. G.; Patrocinio, A. O. T.; Iha, N. Y. M.; Templeton, J. L.; Meyer, T. J., Making Oxygen with Ruthenium Complexes. *Accounts of Chemical Research* **2009,** *42* (12), 1954-1965.

33. Fagnoni, M.; Dondi, D.; Ravelli, D.; Albini, A., Photocatalysis for the formation of the C-C bond. *Chemical Reviews* **2007,** *107* (6), 2725-2756.

34. Lee, C. L. K.; Loh, T. P., Gram-scale synthesis of (-)-epibatidine. *Organic Letters* **2005,** *7* (14), 2965-2967.

35. Reiter, L. W.; Ruppert, P. H., BEHAVIORAL TOXICITY OF TRIALKYLTIN COMPOUNDS - A REVIEW. *Neurotoxicology* **1984,** *5* (2), 177-186.

36. Narayanam, J. M. R.; Tucker, J. W.; Stephenson, C. R. J., Electron-Transfer Photoredox Catalysis: Development of a Tin-Free Reductive Dehalogenatioin Reaction. *Journal of the American Chemical Society* **2009,** *131* (25), 8756-+.

37. Pac, C.; Ihama, M.; Yasuda, M.; Miyauchi, Y.; Sakurai, H., RU(BPY)32+-MEDIATED PHOTO-REDUCTION OF OLEFINS WITH 1-BENZYL-1,4-DIHYDRONICOTINAMIDE - A MECHANISTIC PROBE FOR ELECTRON-TRANSFER REACTIONS OF NAD(P)H-MODEL COMPOUNDS. *Journal of the American Chemical Society* **1981,** *103* (21), 6495-6497.

38. Millett, F.; Durham, B., Design of photoactive ruthenium complexes to study interprotein electron transfer. *Biochemistry* **2002,** *41* (38), 11315-11324.

39. Prier, C. K.; Rankic, D. A.; MacMillan, D. W. C., Visible Light Photoredox Catalysis with Transition Metal Complexes: Applications in Organic Synthesis. *Chemical Reviews* **2013,** *113* (7), 5322-5363.

40. Puckett, L. Photochemistry of a Series of Weakly Coupled Dinuclear Ruthenium(II) Cpmplexes. University of Arkansas, 2015.

41. Toyota, S.; Goto, A.; Kaneko, K.; Umetani, T., Syntheses, spectroscopic properties, and CU(I) complexes of all possible symmetric BI-1,10-phenanthrolines. *Heterocycles* **2005,** *65* (3), 551-562.

42. Aguirre, P.; Zolezzi, S.; Parada, J.; Bunel, E.; Moya, S. A.; Sariego, R., Ruthenium carbonyl complexes in catalytic epoxidation of olefins co-catalyzed by isobutyl-aldehyde. *Applied Organometallic Chemistry* **2006,** *20* (4), 260-263.

43. (a) Spiccia, L.; Deacon, G. B.; Kepert, C. M., Synthetic routes to homoleptic and heteroleptic ruthenium(II) complexes incorporating bidentate imine ligands. *Coordination Chemistry Reviews* **2004,** *248* (13-14), 1329-1341; (b) Thomas, N. C., SUBSTITUTED RUTHENIUM CARBONYL HALIDES. *Coordination Chemistry Reviews* **1986,** *70*, 121-156.

44. Satoshi Nishigaki, H. Y. a. K. N., The Crystal and Molecular Structure of o-Phenanthroline. *Acta Cryst* **1978,** *B34*, 875-879.

45. Jawher Abdelhak, S. N. C. a. M. F. Z., Synthesis, characterization and crystal structure of new cobalt (III) complex: [Tris(1,10-phenanthroline-κ2N,N') Cobalt (III)] trinitrate monohydrate [Co(C12H8N2)3](NO3)3.H2O. *Mediterranean Journal of Chemistry* **2014,** *3(1)*, 738-745.

46. Bolletta, F.; Juris, A.; Maestri, M.; Sandrini, D., QUANTUM YIELD OF FORMATION OF THE LOWEST EXCITED-STATE OF RU(BPY)3(2+) AND RU(PHEN)3(2+). *Inorganica Chimica Acta-Letters* **1980,** *44* (4), L175-L176.

47. Neumannspallart, M.; Kalyanasundaram, K.; Gratzel, C.; Gratzel, M., RUTHENIUM DIOXIDE ELECTRODES AS SUITABLE ANODES FOR WATER PHOTOLYSIS. *Helvetica Chimica Acta* **1980,** *63* (5), 1111-1118.